

Causally-Aware Information Bottleneck for Domain Adaptation

Mohammad Ali Javidian

Department of Computer Science
Appalachian State University

javidianma@appstate.edu

Abstract

We tackle a common domain adaptation setting in causal systems. In this setting, the target variable is observed in the source domain but is entirely missing in the target domain. We aim to impute the target variable in the target domain from the remaining observed variables under various shifts. We frame this as learning a compact, mechanism-stable representation. This representation preserves information relevant for predicting the target while discarding spurious variation. For linear Gaussian causal models, we derive a closed-form Gaussian Information Bottleneck (GIB) solution. This solution reduces to a canonical correlation analysis (CCA)-style projection and offers Directed Acyclic Graph (DAG)-aware options when desired. For nonlinear or non-Gaussian data, we introduce a Variational Information Bottleneck (VIB) encoder–predictor. This approach scales to high dimensions and can be trained on source data and deployed zero-shot to the target domain. Across synthetic and real datasets, our approach consistently attains accurate imputations, supporting practical use in high-dimensional causal models and furnishing a unified, lightweight toolkit for causal domain adaptation.

1 Introduction

Modern prediction systems are rarely deployed in the same environment in which they were trained. Shifts in demographics, sensors, or policies alter the joint distribution of variables and erode accuracy. This motivates *domain adaptation*: transferring knowledge from a labeled *source* to an unlabeled or partially labeled *target* whose distribution differs. In fact, when a model trained in one environment fails in another, the culprit is rarely randomness; it is a change in the data-generating *mechanisms*. Two archetypal shifts capture common failures: Under *covariate shift*, the context distribution changes while the conditional mechanism remains fixed, i.e., $P(X)$ (or $P_{\text{source}}(X) \neq P_{\text{target}}(X)$) varies but $P(Y | X)$ is invariant Shimodaira (2000); Sugiyama et al. (2008); Johansson et al. (2019). Under *target (label) shift*, the marginal $P(Y)$ differs whereas $P(X | Y)$ is stable Storkey (2009); Zhang et al. (2013); Lipton et al. (2018). Broader taxonomies and theoretical results can be found in Redko et al. (2019). We focus on settings where the target variable is *missing in the target domain* and the goal is to impute it reliably under covariate, target, or constrained generalized target shift where the marginal $P(Y)$ changes, and the conditional $P(X|Y)$ changes with constraints.

Causality as a stabilizer. Causal structure provides a lens to separate robust signal from spurious correlation. In theory, causal inference tools aim to protect against instability by aligning with the graph of cause and effect. For example, *selection diagrams* formalize differences between populations and support *transportability* via do-calculus Pearl (2009); Bareinboim & Pearl (2011; 2012; 2014); Correa & Bareinboim (2019). *Invariant causal prediction* (ICP) searches for subsets whose residuals are stable across environments Peters et al. (2016); Pfister et al. (2019a;b), while *graph surgery* proactively removes unstable mechanisms Subbaswamy & Saria (2018; 2019). A complementary line frames adaptation as *graph pruning* to select predictors that yield invariant conditionals Magliacane et al. (2018); Rojas-Carulla et al. (2018); Kouw & Loog (2019). Despite their guarantees, these methods often require causal effect estimation or counterfactual reasoning, can be conservative (trading variance for zero transfer bias), and may struggle to scale. More

recent advances in *invariant risk minimization* Arjovsky et al. (2019) and deep generative approaches for causal representation learning Krueger et al. (2021); Lv et al. (2022) promise improved robustness to unseen shifts.

Our view: compact, mechanism-stable representations. In this paper, we formulate adaptation as learning a *mechanism-stable* summary: a low-dimensional representation that retains target-relevant information and suppresses spurious variation. We design a *DAG-aware information bottleneck* that aligns the encoder with the causal structure while explicitly compressing the observed variables X into a bottleneck U , which preserves valuable information for predicting T and discards nuisance variation. For this purpose, we will use the DAG structure information (e.g., parents/Markov blanket) to focus the encoder on stable mechanisms and avoid unstable paths. This approach yields a representation that is small, causally grounded, and stable across domains, with formal guarantees in the Gaussian case and distribution-free justifications for the nonlinear/non-Gaussian regime.

Motivating example (high-dimensional spurious block; MB-invariance holds). We consider a linear-Gaussian SEM designed to isolate the benefit of restricting the bottleneck to $\text{MB}(T)$ under *domain shift that does not perturb the target mechanism*. The causal structure is shown in Fig. 1. Let $C = (C_1, \dots, C_k)$ denote a small set of stable causal drivers of T , $S = (S_1, \dots, S_m)$ a high-dimensional block of *spurious proxies* whose relationship to C changes across domains, and $N = (N_1, \dots, N_r)$ a nuisance block affected by the domain but irrelevant to T . In the *source* domain, the mechanisms are

$$\begin{aligned} C_i &\sim \mathcal{N}(0, 1), \quad i = 1, \dots, k, \\ T &= w^\top C + \varepsilon_T, \\ S_j &= a_0 (w^\top C) + \varepsilon_{S_j}, \quad j = 1, \dots, m, \\ N_\ell &= b_0 + \varepsilon_{N_\ell}, \quad \ell = 1, \dots, r, \end{aligned}$$

with mutually independent noises $\varepsilon_T \sim \mathcal{N}(0, \sigma_T^2)$, $\varepsilon_{S_j} \sim \mathcal{N}(0, \sigma_{S_j}^2)$, $\varepsilon_{N_\ell} \sim \mathcal{N}(0, \sigma_{N_\ell}^2)$, and a fixed $w \in \mathbb{R}^k$. The Markov blanket of the target is therefore $\text{MB}(T) = \{C_1, \dots, C_k\}$, since T has parents C and no observed children or spouses in this example.

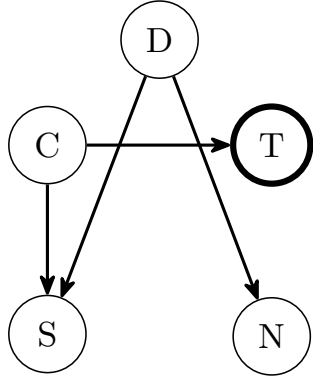


Figure 1: Causal DAG underlying the motivating example. **C**: stable causal drivers of T (the Markov blanket); **S**: high-dimensional spurious proxy block whose conditional distribution shifts with **D**; **N**: nuisance block affected by **D** but irrelevant to T . The target mechanism $p(T | C)$ is invariant across domains.

Shift scenario. We consider a *large* shift in the target domain that changes only non-blanket mechanisms. Specifically, in the *target* domain we keep the target mechanism unchanged,

$$T = w^\top C + \varepsilon_T \quad (\text{same } w, \sigma_T^2),$$

but we alter the proxy and nuisance blocks via domain-dependent parameters

$$\begin{aligned} S_j &= a_1 (w^\top C) + \varepsilon_{S_j}, \quad j = 1, \dots, m, \\ N_\ell &= b_1 + \varepsilon_{N_\ell}, \quad \ell = 1, \dots, r, \end{aligned}$$

with $a_1 \neq a_0$ (in our experiments, a sign flip $a_0 = +1$, $a_1 = -1$) and $b_1 \neq b_0$. Crucially, this construction preserves

$$p_s(T | \text{MB}(T)) = p_s(T | C) = p_t(T | C) = p_t(T | \text{MB}(T)),$$

so the risk-transfer identity under MB-invariance applies, while the *global* input distribution shifts substantially.

As before, T is unobserved at deployment in the target domain. We compare two approaches for predicting (imputing) T under this shift: (a) the Markov blanket Gaussian Information Bottleneck (GIB), and (b) the global GIB (see Sect. 4). Results are reported in Table 1 and Fig. 2.

Table 1: Average error metrics under spurious-proxy shift (MB-invariance holds) for the motivating example.

Method	MAE	RMSE	R^2
Markov Blanket GIB	0.82	1.02	0.82
Global GIB	7.96	10.03	-15.89

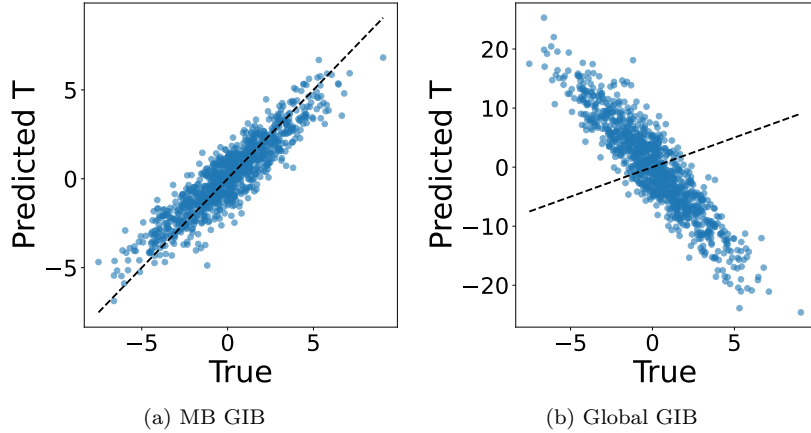


Figure 2: True vs. predicted (imputed) T under the spurious-proxy shift. The Markov-blanket GIB remains accurate because it encodes only $C = \text{MB}(T)$, for which $p_s(T | C) = p_t(T | C)$ holds exactly. In contrast, the global GIB collapses: the high-dimensional proxy block S dominates the bottleneck in the source, but its relationship to T reverses in the target (sign flip), yielding anti-predictive representations and large negative R^2 .

Discussion. This example highlights a sharp, theory-aligned separation between global and Markov-blanket scopes. Because the target mechanism is invariant, restricting the encoder to $\text{MB}(T) = \{C_1, \dots, C_k\}$ preserves precisely the information required for transfer, and the MB GIB achieves strong target performance ($R^2 \approx 0.82$). By contrast, the global encoder has access to a large set of non-blanket variables S that are highly predictive in the source yet shift substantially across domains; under a tight bottleneck, the global GIB preferentially compresses these dominant proxy directions, leading to systematic failure in the target (RMSE 10.03, $R^2 = -15.89$). Taken together, the results demonstrate that a *DAG-aware Information Bottleneck* with a Markov-blanket encoder can provide a principled and practically robust solution to domain adaptation, precisely in the regime where the MB-invariance guarantee applies.

We summarize our main contributions as follows:

- **Mechanism-stable representations (Section 2 and 4).** We propose a *DAG-aware Information Bottleneck* that learns a low-dimensional summary (U) aligned with the causal structure, preserving information necessary for the target variable (T) while suppressing shift-prone nuisance variation.
- **DAG-guided encoders (Section 2 and 4).** We instantiate a practical encoder, *Markov-blanket*, that leverage known graph structure (i.e., Markov blanket of T) to target mechanism-stable pathways and avoid unstable paths.

- **Theory.** We provide formal guarantees in the Gaussian setting (Section 4.1) and distribution-agnostic justification for nonlinear/non-Gaussian regimes (Section 4.2), supporting the stability of the learned representations across domains.
- **Empirics (Section 5).** On synthetic and real datasets, the proposed method achieves accurate imputations under severe shifts, substantially outperforming a fit-on-source Bayesian network baseline; the Markov-blanket encoder offers a small but consistent edge when the prior on (T) is perturbed.

2 Related Work

Origins and Early Development of the Information Bottleneck The Information Bottleneck (IB) was introduced by Tishby, Pereira, and Bialek (1999) Tishby et al. (2000) as a principled way to extract task-relevant structure from data: learn a stochastic code (T) of (X) that maximizes mutual information with a target (Y) while compressing information about (X) . Early work established the Lagrangian trade-off $I(X; T) - \beta I(T; Y)$, the self-consistent IB equations, and the “information curve” characterizing relevance vs. compression. Soon after, efficient clustering algorithms appeared—most notably the Agglomerative IB (AIB) of Slonim and Tishby—which applied IB to unsupervised/text settings and gave scalable heuristics for discrete variables Slonim & Tishby (1999); Slonim et al. (2001). On the theory side, Gaussian IB Chechik et al. (2003) provided closed-form solutions for jointly Gaussian variables and linked IB to canonical correlation analysis and rate-distortion theory. Variants such as multi-variate IB Slonim et al. (2006) and deterministic annealing schemes broadened applicability, and by the mid-2000s IB had become a unifying lens for representation learning, lossy compression with task-aware distortions, and information-theoretic clustering—setting the stage for later variational/deep renditions.

From Theory to Deep Learning: The Variational Turn of IB The next wave of IB research made the framework practical for high-dimensional data by introducing variational surrogates and neural parameterizations. The *Variational Information Bottleneck* casts IB as a stochastic encoder-decoder trained with the reparameterization trick, optimizing a predictive loss plus a KL penalty to a simple prior; the trade-off coefficient β becomes a tunable “information budget” Alemi et al. (2016). This bridged IB with modern generative modeling—most visibly β -VAE as an unsupervised, rate-distortion analogue Burgess et al. (2018)—and enabled end-to-end training on images, text, and speech. In parallel, deterministic and annealed variants (e.g., the Deterministic Information Bottleneck) and “information plane” studies explored how compression emerges during deep training, sparking debate about generalization and the role of noise Strouse & Schwab (2017); Tishby & Zaslavsky (2015). Subsequent work broadened IB’s scope: nonlinear/non-Gaussian decoders and tighter variational bounds on mutual information Poole et al. (2019), connections to dropout and noise injection as implicit bottlenecks Achille & Soatto (2018), and task-aware objectives such as the Conditional Entropy Bottleneck for robust prediction Fischer (2020).

IB and Causal Inference. Recent work integrates the Information Bottleneck with causal goals to obtain representations that are stable under interventions and distribution shift. A formal “causal IB” reframes sufficiency in interventional terms, proposing an objective that *compresses* X while *preserving causal control* of a target Y —yielding a CIB Lagrangian and an axiomatic notion of optimal causal variable abstractions that can be reasoned about with backdoor adjustment and without full DAG knowledge Simoes et al. (2025). Beyond interventional sufficiency, causal IB ideas have been used to *separate robust (causal) from non-robust (spurious/style)* features via instrumental-variable style interventions, improving adversarial robustness by down-weighting non-causal signal within the bottleneck Hua et al. (2022). For domain generalization, *Invariant Information Bottleneck* (IIB) casts invariant causal prediction in mutual-information terms and regularizes $I(Z; X)$ to avoid pseudo-invariant and geometrically skewed shortcuts, delivering tractable variational losses and consistent OOD gains Li et al. (2022). Together, these strands position IB as a bridge between predictive compression and causal transportability: learn minimal, interventionally sufficient codes that transfer across environments while suppressing spurious variability.

How our MB–GIB and MB–VIB differ. Our approach is *DAG-aware and node-specific*: we place the bottleneck downstream of the *Markov blanket of the target T* and learn summaries solely from $\text{MB}(T)$ (or

parents) to impute/predict T under shift. In the linear-Gaussian case, MB-GIB is a *closed-form* IB/CCA solution with an explicit blanket constraint; MB-VIB is its *nonlinear, non-Gaussian* variational counterpart (stochastic encoder; Student- t /Laplace heads). This differs from *Causal IB* Simoes et al. (2025), which optimizes an interventional sufficiency objective to produce *causal abstractions* (possibly without full DAG knowledge) aimed at preserving *causal control* rather than enforcing a fixed blanket restriction. It also differs from adversarial-robustness uses of CIB Hua et al. (2022), which introduce IV-style interventions/adversarial criteria to separate robust from non-robust features, whereas we exploit *known causal structure* to preclude non-blanket pathways a priori. Finally, unlike *Invariant Information Bottleneck* Li et al. (2022), which regularizes mutual information to induce environment-level invariance (often requiring multiple environments or environment labels), our invariance comes from *structural* restriction: by confining the encoder to $\text{MB}(T)$, we keep mechanism-stable, T -relevant signals and discard context- or downstream-induced variability. Practically, this yields a simple pipeline: (i) graph-constrained encoder (MB or parents), (ii) closed-form GIB or variational VIB training on a *single* source environment, and (iii) zero-shot deployment to shifted targets, without interventional data, adversarial training, or multi-environment supervision.

When MB-GIB / MB-VIB are most useful. Our DAG-aware bottlenecks are most powerful when a (partial) graph around the target T is known, training comes from a *single* source environment, and deployment faces *contextual* shifts while mechanisms are stable. They are especially effective when T is unobserved at test time, data are limited (closed-form MB-GIB is sample-efficient), or robustness is critical: by restricting the encoder to $\text{MB}(T)$, they transfer zero-shot, avoid spurious downstream paths, and require neither interventional data nor multi-environment supervision.

3 Problem Statement

We formalize domain adaptation for imputing a *target variable* $T = X_t$ across environments when only *local causal information* around T is available and data may be non-Gaussian.

Data and observables. Let $X = (X_1, \dots, X_p)$ be p observed variables. We observe a *source* dataset with T present,

$$\mathcal{D}_s = \{X_s^{(i)}\}_{i=1}^{N_s}, \quad X_s^{(i)} = (X_{1,s}^{(i)}, \dots, X_{p,s}^{(i)}),$$

and a *target* dataset in which T is entirely missing,

$$\mathcal{D}_t^{\text{obs}} = \{X_{t,-t}^{(j)}\}_{j=1}^{N_t}, \quad X_{t,-t}^{(j)} = (X_{1,t}^{(j)}, \dots, X_{t-1,t}^{(j)}, X_{t+1,t}^{(j)}, \dots, X_{p,t}^{(j)}).$$

Graphical knowledge: Markov blanket of T . We *do not assume* the full DAG is known. Instead, we assume access to (or can reliably estimate) the *Markov blanket* of T in some underlying DAG \mathcal{G} :

$$\text{MB}(T) = \text{Pa}(T) \cup \text{Ch}(T) \cup \bigcup_{C \in \text{Ch}(T)} \text{Pa}(C) \setminus \{T\},$$

i.e., the union of T 's parents, its children, and the parents of those children (spouses). By the local Markov property, $T \perp X \setminus (\text{MB}(T) \cup \{T\}) \mid \text{MB}(T)$. In words, conditioning on $\text{MB}(T)$ renders T independent of all remaining nodes.

Model class (beyond Gaussian). We allow *arbitrary* (possibly nonlinear, non-Gaussian) structural mechanisms and noise distributions; no linearity or Gaussianity is required. Throughout, we make no parametric restrictions on the joint distribution other than the blanket conditional independence above.

Shift model (MB invariance). Source and target environments may differ (covariate/target shifts) in the marginals of exogenous or downstream variables and in joint correlations outside the blanket. Our sole stability assumption is *MB invariance*:

$$p_s(T \mid \text{MB}(T)) = p_t(T \mid \text{MB}(T)),$$

i.e., the conditional law of T given its blanket is unchanged across domains. Under this assumption, shifts outside $\text{MB}(T)$ cannot alter $p(T | \text{MB}(T))$ by conditional independence; shifts *within* $\text{MB}(T)$ may occur in the marginals of blanket variables but not in the mechanism linking T to its blanket.

Task. Let $M := \text{MB}(T)$ be the index set of blanket variables, and write $X_M = (X_k)_{k \in M}$. For the j -th target sample, denote its blanket subvector by $x_{M,t}^{(j)} := (X_{k,t}^{(j)})_{k \in M}$. Given $(\mathcal{D}_s, \mathcal{D}_t^{\text{obs}}, M)$ and the MB-invariance assumption $p_s(T | X_M) = p_t(T | X_M)$, we impute the missing targets via the (source-trained) Bayes predictor

$$\hat{T}^{(j)} = \mathbb{E}_{p_s}[T | X_M = x_{M,t}^{(j)}], \quad j = 1, \dots, N_t.$$

The equality of conditionals ensures *zero-shot transfer* from source to target. Practically, we estimate this conditional with a *DAG-aware Information Bottleneck* restricted to inputs $X_S \in \text{MB}(T)$: a closed-form, sample-efficient linear MB–GIB, and a nonlinear MB–VIB (stochastic encoder/decoder) for non-Gaussian, nonlinear settings.

4 Methodology and Theoretical Results

We develop a *DAG-aware Information Bottleneck* pipeline tailored to imputing an unobserved target T under domain shift using only local causal knowledge. Our methodology enforces a structural input constraint—encoders see either the parents $\text{Pa}(T)$ or the Markov blanket $\text{MB}(T)$ —and exploits the *MB-invariance* assumption $p_s(T | X_{\text{MB}}) = p_t(T | X_{\text{MB}})$ to enable zero-shot transfer. Concretely, we present (i) a closed-form **MB–GIB** for the linear–Gaussian case, where the GIB subspace equals CCA directions and we prove that restricting to $\text{MB}(T)$ is *lossless* relative to using all non- T variables; and (ii) a **MB–VIB** with stochastic encoders and flexible (Laplace/Student- t) decoders for nonlinear, non-Gaussian settings, trained by a predictive loss plus a KL compression term. On the theory side, we show (a) equivalence of global and MB-restricted GIB spectra in the Gaussian case and a block-matrix proof that all optimal directions lie in the lifted MB(T) subspace; (b) identifiability of the population predictor $\mathbb{E}[T | X_{\text{MB}}]$ from source data and its risk preservation in the target domain under MB-invariance; and (c) finite-sample guarantees that the IB estimators concentrate around the population conditional, with robustness to shifts outside the blanket. Together, these results justify using $\text{MB}(T)$ as a *structurally minimal* and *transfer-stable* interface for bottleneck learning, and they motivate our practical algorithms that remain sample-efficient (MB–GIB) yet expressive (MB–VIB) across a wide range of data regimes.

4.1 MB–GIB: Closed-Form Solution and Lossless Restriction (Gaussian)

In the linear–Gaussian case, whitening X_S and T turns the IB tradeoff into finding directions in X_S that are *maximally correlated* with T . This is exactly canonical correlation analysis (CCA): solve a symmetric eigenproblem for the operator $\Omega_{X_S} = \Sigma_{X_S X_S}^{-1/2} \Sigma_{X_S T} \Sigma_{T T}^{-1} \Sigma_{T X_S} \Sigma_{X_S X_S}^{-1/2}$, take its top d eigenvectors, unwhiten to get W , and encode $Z = W^\top X_S$. Because the model is Gaussian and linear, these Z are *sufficient statistics* for predicting T : no other linear combination of X_S carries additional predictive information once Z is known. The decoder is just the optimal linear predictor of T from Z (ordinary least squares): $\hat{T} = B^\top Z$ with $B = (Z^\top Z)^{-1} Z^\top T$. The IB parameter β acts as a *spectral threshold*: only CCA directions with squared canonical correlation above a β -dependent cutoff are kept (equivalently, choose d to retain the leading spectrum). Under the Markov-blanket restriction $X_S = \text{MB}(T)$, the nonzero spectrum matches the global one, so this closed-form encoder/decoder is *lossless* relative to using all non- T variables.

Lossless restriction theorem (informal). Let $X = (X_{-t}, T)$ and $M = \text{MB}(T)$. In the Gaussian case, assuming $T \perp X \setminus (M \cup \{T\}) | M$, the nonzero spectra of the global CCA operator Ω_X and the blanket operator Ω_M coincide, and every global CCA direction lies in the lifted subspace generated by M . Hence restricting the encoder to $\text{MB}(T)$ is *without loss* for any bottleneck dimension d .

Proof sketch. Using the Markov-blanket factorization $\Sigma_{XT} = L \Sigma_{MT}$ with $L = [I; B]$, one shows $L^\top \Sigma_{XX}^{-1} L = \Sigma_{MM}^{-1}$. This yields $S_X = Q S_M$ with Q column-orthonormal, so S_X and S_M have identical singular values, implying equal nonzero spectra and lifted eigenvectors (details in the supplement).

Practical recipe and cost. Compute empirical covariances on source (X_S, T) , form Ω_{X_S} , take its top d eigenvectors to obtain W , and fit B by least squares from Z to T . Complexity is $O(n|X_S|^2 + |X_S|^3)$, typically small since $|X_S| = |M|$. At test time, encode $z = W^\top x_{S,t}$ and predict $\hat{T} = B^\top z$.

4.2 MB–VIB: Nonlinear, Non-Gaussian Bottleneck (Practical Variant)

When relationships are nonlinear or noises are non-Gaussian, we use a variational bottleneck restricted to $X_S \in \text{MB}(T)$. The encoder is a stochastic map $q_\phi(z | x_S)$ (neural mean/variance with reparameterization), the decoder a flexible likelihood $q_\theta(t | z)$ (Gaussian/Laplace/Student- t as appropriate). We train on source pairs (x_S, t) by minimizing

$$\begin{aligned}\mathcal{L}_{\text{VIB}}(\phi, \theta) = & \mathbb{E}_{(x_S, t)} \mathbb{E}_{z \sim q_\phi(\cdot | x_S)} [-\log q_\theta(t | z)] \\ & + \beta \mathbb{E}_{x_S} D_{\text{KL}}(q_\phi(z | x_S) \| r(z)).\end{aligned}$$

with a simple prior $r(z)$ (e.g., $\mathcal{N}(0, I)$). The first term fits a predictive decoder for T ; the KL controls information $I(X_S; Z)$ and thus shrinks nuisance variability that does not help predict T . The DAG-aware input restriction prevents leakage from non-blanket pathways, aligning the learned representation with the transfer-stable mechanism $p(T | X_M)$.

Design choices. (i) Likelihood: choose q_θ to match the target type (e.g., Student- t for heavy tails); (ii) Capacity: adjust z -dim and β to trade accuracy for robustness; (iii) Stability: standardization, early stopping, and prior tempering improve optimization. *Deployment* is simple: encode $z = f_\phi(x_{S,t})$ from target inputs restricted to X_S , then output $\hat{T} = \mathbb{E}[T | z]$ (regression) or $\arg \max_y q_\theta(y | z)$ (classification). The blanket restriction prevents leakage from non-blanket pathways, while the variational bottleneck captures nonlinear predictors that remain stable under shifts outside $\text{MB}(T)$.

4.3 Transfer Guarantees under MB Invariance

We give high-level guarantees for blanket-restricted IB predictors; proofs and regularity conditions appear in the supplement.

Identifiability (population). Let $M = \text{MB}(T)$ and assume $p_s(T | X_M) = p_t(T | X_M)$. Then the Bayes rule

$$g^*(x_M) = \mathbb{E}_{p_s}[T | X_M = x_M] = \mathbb{E}_{p_t}[T | X_M = x_M]$$

is identifiable from source data alone and is target-optimal conditional on X_M .

Risk preservation (zero-shot). For squared or log loss, any estimator \hat{g} trained on source pairs (X_M, T) and applied to target inputs satisfies

$$\mathcal{R}_t(\hat{g}) - \mathcal{R}_t(g^*) = \mathcal{R}_s(\hat{g}) - \mathcal{R}_s(g^*),$$

so source excess risk transfers verbatim to the target. In particular: (i) *MB–GIB losslessness* in the Gaussian/linear case (Sec. 4.1) shows restricting inputs to X_M is without loss for any bottleneck dimension; (ii) *MB–VIB consistency* (Sec. 4.2) implies target consistency whenever source risk vanishes; and (iii) by $T \perp X \setminus (M \cup \{T\}) | X_M$, shifts outside M cannot change the optimal predictor.

Practical Considerations (1) *Checking MB invariance.* Compare source vs. target residuals or decoder log-likelihoods of $\hat{g}(X_{M,t})$; systematic shifts flag drift in $p(T | X_M)$. (2) *Estimating M when unknown.* Run local discovery around T (parents/children/spouses) and prune via conditional-independence tests on the source; validate by goodness-of-fit of $p_s(T | X_M)$ and stability of residuals in target. (3) *Tuning.* Increase β and decrease d_z for robustness; select decoder likelihood to match tails (Gaussian/Laplace/Student- t).

4.4 Finite-Sample Guarantees and Robustness

We now make the finite-sample and robustness claims in Secs. 4.1–4.3 explicit. The goal is twofold: (i) quantify how the *MB–GIB* estimator (which is computed from empirical covariances) concentrates around its population solution (equivalently, around the population conditional $g^*(x_M) = \mathbb{E}[T \mid X_M = x_M]$); and (ii) formalize robustness under distribution shift, clarifying which guarantees require exact MB invariance and which extend to small violations.

Setup and notation. Let $M = \text{MB}(T)$ and denote $X_M \in \mathbb{R}^p$ with $p := |M|$. We observe i.i.d. *source* samples $\{(X_{M,i}, T_i)\}_{i=1}^n \sim p_s(X_M, T)$. Let $Z := (X_M^\top, T)^\top \in \mathbb{R}^{p+1}$ with population covariance

$$\Sigma := \text{Cov}(Z) = \begin{pmatrix} \Sigma_{XX} & \Sigma_{XT} \\ \Sigma_{TX} & \Sigma_{TT} \end{pmatrix}, \quad \widehat{\Sigma} := \text{Cov}_n(Z)$$

the corresponding sample covariance (with delta degrees of freedom $ddof = 1$). In the Gaussian/linear regime of Sec. 4.1, the MB–GIB directions are the top eigenvectors of the CCA operator

$$\Omega_M := \Sigma_{XX}^{-1/2} \Sigma_{XT} \Sigma_{TT}^{-1} \Sigma_{TX} \Sigma_{XX}^{-1/2} \in \mathbb{R}^{p \times p},$$

and the empirical estimator replaces Σ by $\widehat{\Sigma}$, yielding $\widehat{\Omega}_M$. Let $U_\star \in \mathbb{R}^{p \times d}$ collect the top d eigenvectors of Ω_M , and \widehat{U} those of $\widehat{\Omega}_M$. We measure subspace error using the principal-angle quantity $\|\sin \Theta(\widehat{U}, U_\star)\|_{\text{op}}$, and write $\Pi_\star = U_\star U_\star^\top$, $\widehat{\Pi} = \widehat{U} \widehat{U}^\top$ for the projectors.

Assumptions (finite-sample MB–GIB). The following conditions are standard in non-asymptotic covariance and spectral analysis, and they are satisfied by the linear–Gaussian SEMs used in our experiments.

Assumption 1 (Joint sub-Gaussian source law). *Let $Z := (X_M^\top, T)^\top \in \mathbb{R}^{p+1}$ denote the source random vector with $\mathbb{E}(Z) = 0$ and covariance Σ . We assume Z is K -sub-Gaussian in the standard (joint) sense:*

$$\|Z\|_{\psi_2} := \sup_{\|u\|_2=1} \|u^\top Z\|_{\psi_2} \leq K,$$

where $\|\cdot\|_{\psi_2}$ is the sub-Gaussian Orlicz norm. (In particular, the linear–Gaussian SEM case satisfies this condition.)

Assumption 2 (Blanket covariance conditioning). *The blanket covariance is well-conditioned: $\lambda_{\min}(\Sigma_{X_M X_M}) \geq \lambda_0 > 0$ and $\lambda_{\max}(\Sigma_{X_M X_M}) \leq \Lambda_0 < \infty$.*

Assumption 3 (Spectral gap for the retained CCA spectrum). *Let $\lambda_1 \geq \dots \geq \lambda_p \geq 0$ be the eigenvalues of Ω_M . For the chosen bottleneck dimension d , there is an eigengap $\gamma := \lambda_d - \lambda_{d+1} > 0$ (with $\lambda_{p+1} := 0$).*

(A) Concentration of empirical covariances. Theorem 1 quantifies estimation error of the covariance blocks used by MB–GIB.

Theorem 1 (Covariance concentration). *Under Assumption 1, for any $\delta \in (0, 1)$, with probability at least $1 - \delta$,*

$$\|\widehat{\Sigma} - \Sigma\|_{\text{op}} \leq c K^2 \left(\sqrt{\frac{p+1 + \log(1/\delta)}{n}} + \frac{p+1 + \log(1/\delta)}{n} \right),$$

where $c > 0$ is a universal constant. In particular, the same bound holds for each block $\widehat{\Sigma}_{XX}, \widehat{\Sigma}_{XT}, \widehat{\Sigma}_{TT}$.

(B) Finite-sample stability of the MB–GIB spectrum. Theorem 2 translates covariance error into spectral (subspace) error for the CCA/GIB directions, with the eigengap γ controlling sensitivity.

Theorem 2 (MB–GIB spectral/subspace concentration). *Assume Assumptions 1–3. Let U_\star and \widehat{U} be the population and empirical top- d eigenspaces of Ω_M and $\widehat{\Omega}_M$, respectively. Then, with probability at least $1 - \delta$,*

$$\|\sin \Theta(\widehat{U}, U_\star)\|_{\text{op}} \leq \frac{C}{\gamma} \|\widehat{\Omega}_M - \Omega_M\|_{\text{op}} \leq \frac{C'}{\gamma} \|\widehat{\Sigma} - \Sigma\|_{\text{op}} \lesssim \frac{K^2}{\gamma} \sqrt{\frac{p + \log(1/\delta)}{n}},$$

where $C, C' > 0$ depend only on the conditioning constants λ_0, Λ_0 (Assumption 2). Equivalently, $\|\widehat{\Pi} - \Pi_\star\|_{\text{op}} \leq 2\|\sin \Theta(\widehat{U}, U_\star)\|_{\text{op}}$.

(C) Finite-sample excess risk (source) and transfer (target). Theorem 3 yields an explicit $O((p + \log(1/\delta))/n)$ excess-risk rate that depends only on the blanket dimension, formalizing the sample-efficiency benefit of restricting inputs to $\text{MB}(T)$.

Theorem 3 (MB-GIB excess risk rate). *Assume Assumptions 1–2. Let $g^*(x_M) = \mathbb{E}_{p_s}[T \mid X_M = x_M]$ denote the population conditional mean. Let \widehat{g} be the MB-GIB predictor obtained by (i) computing $\widehat{\Omega}_M$, (ii) taking \widehat{U} (or equivalently the corresponding unwhitened W), and (iii) fitting the optimal linear decoder from $Z = \widehat{W}^\top X_M$ to T (Sec. 4.1). Then, for squared loss $\mathcal{R}_s(g) := \mathbb{E}_{p_s}[(T - g(X_M))^2]$, with probability at least $1 - \delta$,*

$$\mathcal{R}_s(\widehat{g}) - \mathcal{R}_s(g^*) \leq C'' \|\widehat{\Sigma} - \Sigma\|_{\text{op}}^2 \lesssim K^4 \frac{p + \log(1/\delta)}{n},$$

where $C'' > 0$ depends only on λ_0, Λ_0 .

Corollaries 1–2 formalize robustness under blanket-based transfer. Under exact MB invariance, the Bayes rule $g^*(x_M) = \mathbb{E}[T \mid X_M = x_M]$ is shared across domains, and the target excess risk is controlled by the source excess risk up to a blanket density-ratio factor ρ_M ; in the special case $p_s(X_M) = p_t(X_M)$ this reduces to an exact equality. Under approximate invariance, departures from the ideal transfer regime are quantified by the conditional-mean mismatch $\Delta(x_M)$ within the blanket, yielding an explicit degradation bound in terms of $\mathbb{E}_{p_t}|\Delta|$ and $\mathbb{E}_{p_t}\Delta^2$. Finally, for the nonlinear MB-VIB variant, analogous non-asymptotic guarantees require explicit capacity control for the encoder/decoder (e.g., Lipschitz/covering-number conditions or PAC-Bayes complexity). Our main theoretical guarantees therefore target MB-GIB (Gaussian/linear), while MB-VIB is a practical extension motivated by the same structural restriction and validated empirically.

Corollary 1 (Zero-shot target bound under MB invariance). *Assume MB invariance $p_s(T \mid X_M) = p_t(T \mid X_M)$, squared loss, and that $p_t(X_M) \ll p_s(X_M)$ with*

$$\rho_M := \text{ess sup}_{x_M} \frac{p_t(x_M)}{p_s(x_M)} < \infty.$$

Then the Bayes predictor

$$g^*(x_M) = \mathbb{E}[T \mid X_M = x_M]$$

is shared across domains and is target-optimal among all predictors measurable w.r.t. X_M . Moreover, for any estimator \widehat{g} (in particular, MB-GIB) we have the conditional excess-risk identity

$$\mathcal{R}_\nu(\widehat{g}) - \mathcal{R}_\nu(g^*) = \mathbb{E}_{p_\nu(X_M)}[(\widehat{g}(X_M) - g^*(X_M))^2], \quad \nu \in \{s, t\}.$$

Consequently,

$$\mathcal{R}_t(\widehat{g}) - \mathcal{R}_t(g^*) \leq \rho_M (\mathcal{R}_s(\widehat{g}) - \mathcal{R}_s(g^*)).$$

In particular, under the assumptions of Theorem 3, with probability at least $1 - \delta$,

$$\mathcal{R}_t(\widehat{g}) - \mathcal{R}_t(g^*) \lesssim \rho_M K^4 \frac{p + \log(1/\delta)}{n}.$$

In the special case $p_s(X_M) = p_t(X_M)$, we have $\rho_M = 1$ and the target and source excess risks coincide.

Corollary 2 (Approximate MB invariance). *Assume squared loss and define the conditional-mean mismatch within the blanket by*

$$\Delta(x_M) := \mathbb{E}_{p_t}[T \mid X_M = x_M] - \mathbb{E}_{p_s}[T \mid X_M = x_M] = g_t^*(x_M) - g_s^*(x_M).$$

Then for any predictor \widehat{g} ,

$$|(\mathcal{R}_t(\widehat{g}) - \mathcal{R}_t(g_t^*)) - \mathbb{E}_{p_t(X_M)}[(\widehat{g}(X_M) - g_s^*(X_M))^2]| \leq 2\mathbb{E}_{p_t}[|\widehat{g}(X_M) - g_s^*(X_M)| |\Delta(X_M)|] + \mathbb{E}_{p_t}[\Delta(X_M)^2].$$

In particular, if shifts occur only outside M then $\Delta \equiv 0$ and

$$\mathcal{R}_t(\widehat{g}) - \mathcal{R}_t(g_t^*) = \mathbb{E}_{p_t(X_M)}[(\widehat{g}(X_M) - g_s^*(X_M))^2],$$

so the target excess risk is exactly the target L_2 error to the source conditional mean. More generally, target degradation is controlled by the blanket mismatch Δ .

4.5 Algorithms and Complexity

Here, we summarize training and deployment for MB–GIB and MB–VIB algorithms:

MB–GIB (linear–Gaussian; closed form). *Input:* source pairs (X_S, T) with $X_S \in \text{MB}(T)$, bottleneck dim. d . *Steps:*

1. Standardize X_S, T on the source; compute $\widehat{\Sigma}_{X_S X_S}, \widehat{\Sigma}_{X_S T}, \widehat{\Sigma}_{T T}$.
2. Form the CCA/IB operator $\widehat{\Omega}_{X_S} = \widehat{\Sigma}_{X_S X_S}^{-1/2} \widehat{\Sigma}_{X_S T} \widehat{\Sigma}_{T T}^{-1} \widehat{\Sigma}_{T X_S} \widehat{\Sigma}_{X_S X_S}^{-1/2}$.
3. Take top- d eigenvectors \widehat{W} of $\widehat{\Omega}_{X_S}$; encode $Z = \widehat{W}^\top X_S$.
4. Fit decoder by least squares: $\widehat{B} = \arg \min_B \|T - Z^\top B\|_2^2$; at test time predict $\widehat{T} = \widehat{B}^\top \widehat{W}^\top x_{S,t}$.

Cost: covariance $O(n|X_S|^2)$; eigen-decomp. $O(|X_S|^3)$; least squares $O(nd^2)$.

MB–VIB (nonlinear, non-Gaussian; variational). *Input:* source pairs (X_S, T) , encoder $q_\phi(z \mid x_S)$, decoder $q_\theta(t \mid z)$, prior $r(z)$, trade-off β , epochs E . *Steps:*

1. Initialize ϕ, θ ; standardize X_S ; choose q_θ (Gaussian/Laplace/Student- t) to match T .
2. For $e = 1, \dots, E$: sample minibatches, draw $z = \mu_\phi(x_S) + \sigma_\phi(x_S) \odot \epsilon$ (reparameterization).
3. Minimize
$$\mathcal{L}_{\text{VIB}} = \mathbb{E}[-\log q_\theta(T \mid Z)] + \beta \mathbb{E}[D_{\text{KL}}(q_\phi(Z \mid X_S) \parallel r(Z))]$$
by SGD; apply early stopping on source validation loss.
4. At test time, encode $z = f_\phi(x_{S,t})$; output $\widehat{T} = \mathbb{E}_{q_\theta}[T \mid z]$ (regression) or $\arg \max_y q_\theta(y \mid z)$ (classification).

Cost: per-epoch $O(n \cdot d_z \cdot H)$ where d_z is latent dimension and H is encoder/decoder width; memory linear in n and model size.

Notes. (1) The *only* inputs to the encoder is $X_S \in \text{MB}(T)$, enforcing the graphical constraint. (2) Choose d or d_z small and increase until validation loss saturates; increase β for more robustness. (3) For heavy-tailed targets, prefer Student- t decoders.

5 Experimental Results

In this section we evaluate DAG-aware Information Bottlenecks under domain shift. We report headline results on three settings: a controlled 7-node SEM with known Markov blanket (for transparent diagnostics), the 64-node *MAGIC-IRRI* Gaussian Bayesian network (benchmark scale; (Scutari, 2016)¹), and a real single-cell signaling dataset from *Sachs et al.* (2005), which provides a stringent biological transfer test where the target (T) is unobserved at deployment. Across all datasets we compare **MB–GIB** and **MB–VIB** against baselines—Bayesian network (BN), pure deep neural network (DNN), and an IIB-style variant Li et al. (2022)—under covariate and generalized target shifts, using MAE/RMSE/(R^2) (mean(\pm)SE over seeds) and runtime. To conserve space, comprehensive *ablations* (scope: Parents/MB/Global, capacity and (β), likelihood, MB misspecification) and *sensitivity* analyses (shift magnitude/type, support mismatch, missingness, (N_s) curves) are conducted on the 7-node SEM and deferred to the supplement; the main text fixes hyperparameters from those sweeps and reports cross-dataset, zero-shot transfer performance. All experiments were executed on a Windows workstation equipped with a 12th Gen Intel(R) Core(TM) i9-12900H 2.50 GHz processor. The source code and experimental scripts for this work are available at the supplementary materials. Code to reproduce the experiments is available at https://github.com/majavid/CDA_IB.

¹The network structure and data are available at <https://www.bnlearn.com/bnrepository/>.

5.1 Simulated Experiments: From Motivationg Example

First, we study a seven-node SEM where contexts C_1, C_2 generate intermediates Z, X , the treatment/latent target T depends on (C_1, X, Z) , and T drives downstreams P, Y . We adopt the *MB-invariance* setting: the Markov blanket $\text{MB}(T) = \{C_1, X, Z, P, Y\}$ is shared across domains, while marginal distributions may shift. We consider two large-shift targets: (i) **covariate shift**, changing only C_2 (e.g., $C_2 \sim \mathcal{N}(5, 2^2)$) with all mechanisms and noise laws fixed; and (ii) **generalized target shift**, changing C_1 (e.g., $C_1 \sim \mathcal{N}(5, 2^2)$) and the disturbance/prior of T via an additive offset and/or inflated ε_T variance. In the target domain, T is unobserved; we impute it zero-shot from observed variables using our DAG-aware bottlenecks, training the encoder/decoder on source pairs (X_S, T) with $X_S \in \text{MB}(T)$, and comparing MB-GIB/MB-VIB to BN, pure DNN, and IIB-style baselines. For the main results, we repeat each case 5 times.

Based on the results, depicted in Fig. 3, the **MB-GIB** model demonstrates consistently superior performance across all evaluation metrics and scenarios. In both the covariate shift and target generation settings, **MB-GIB** achieves the lowest Root Mean Squared Error (RMSE) and Mean Absolute Error (MAE), alongside the highest R^2 score. This success is expected, as the MB-GIB’s Gaussian-to-Gaussian architecture is perfectly matched to the underlying linear-Gaussian causal model, allowing it to analytically identify the optimal predictive information without approximation error. The other models show more variable performance. The **BN** model performs well under the covariate shift but degrades dramatically in the target generation task, where it exhibits the highest error and lowest R^2 score by a significant margin. This failure likely occurs because the model’s flexible encoder overfits to correlational patterns specific to the source data. When the target’s causal mechanism is altered, this non-robust mapping breaks down completely. Similarly, the **MB-VIB**, **IIB-style**, and **PureDNN** models show intermediate performance because their general-purpose neural network components introduce approximation errors and are less effective at isolating the core invariant structure compared to the specialized GIB framework. This highlights that while several models can handle simple covariate shifts, the MB-GIB architecture is uniquely effective for the more challenging generative setting due to its precise alignment with the problem’s structure.

Capacity-compression tradeoffs in MB-VIB. From the heatmaps (lower RMSE is better), the Student- t setting favors a small latent capacity with stronger compression: the best performance occurs at $z_{\text{dim}} = 4$ and $\beta = 0.01$. As capacity grows, β must be tuned carefully— $z = 8, \beta = 0.003$ is competitive, but $z = 8, \beta = 0.01$ and $z = 16, \beta \in \{0.001, 0.01\}$ deteriorate markedly—consistent with heavy tails benefiting from aggressive compression to suppress outliers, while either too much compression (high β) or too little (low β) at large z harms signal retention. Under Laplace noise, a broad low-RMSE band appears for moderate/large capacities $z \in [8, 16]$ with $\beta \in [0.003, 0.01]$; in contrast, $z = 4, \beta = 0.001$ is a clear failure mode. Overall, the results indicate a sweet-spot *coupling* between capacity and compression rather than a single universally optimal choice: heavier tails call for stronger compression and/or smaller z , whereas milder tails work best with moderate compression and larger z . Practically, one should start with a grid such as $z \in \{4, 8, 16\}$, $\beta \in \{0.003, 0.01\}$; if validation error rises when increasing z , raise β slightly, and if error rises when increasing β , reduce β or z . In short, MB-VIB performs best when capacity and compression are balanced to the noise regime—compress harder with heavy tails or small z , and use moderate β with larger z under milder tails.

Sensitivity to support mismatch and missingness. Figure 4 (c), (d) shows that prediction error is dominated by support mismatch rather than missingness. When the stretch factor s (measuring covariate support shift) is near unity, both MB-VIB and MB-GIB achieve low RMSE, with a mild, roughly monotone degradation as the missingness rate m rises from 0 to 0.5. Increasing the mismatch to $s = 1.5$ produces a uniform upward shift in RMSE across all m , indicating that imputation/regularization helps but cannot fully compensate for distributional shift. At severe mismatch $s = 2.0$, error becomes large and essentially insensitive to m , consistent with an extrapolation regime where the predictor leaves the training support. The two variants exhibit nearly identical profiles, suggesting that, for these settings, robustness is limited more by covariate support alignment than by the choice of bottleneck (MB-VIB vs. MB-GIB). Practically, this argues for prioritizing support-alignment techniques (e.g., reweighting, representation alignment, or targeted data collection) before tackling high missingness rates; once support is aligned ($s \approx 1$), the methods remain usable even with substantial missingness ($m \leq 0.5$).

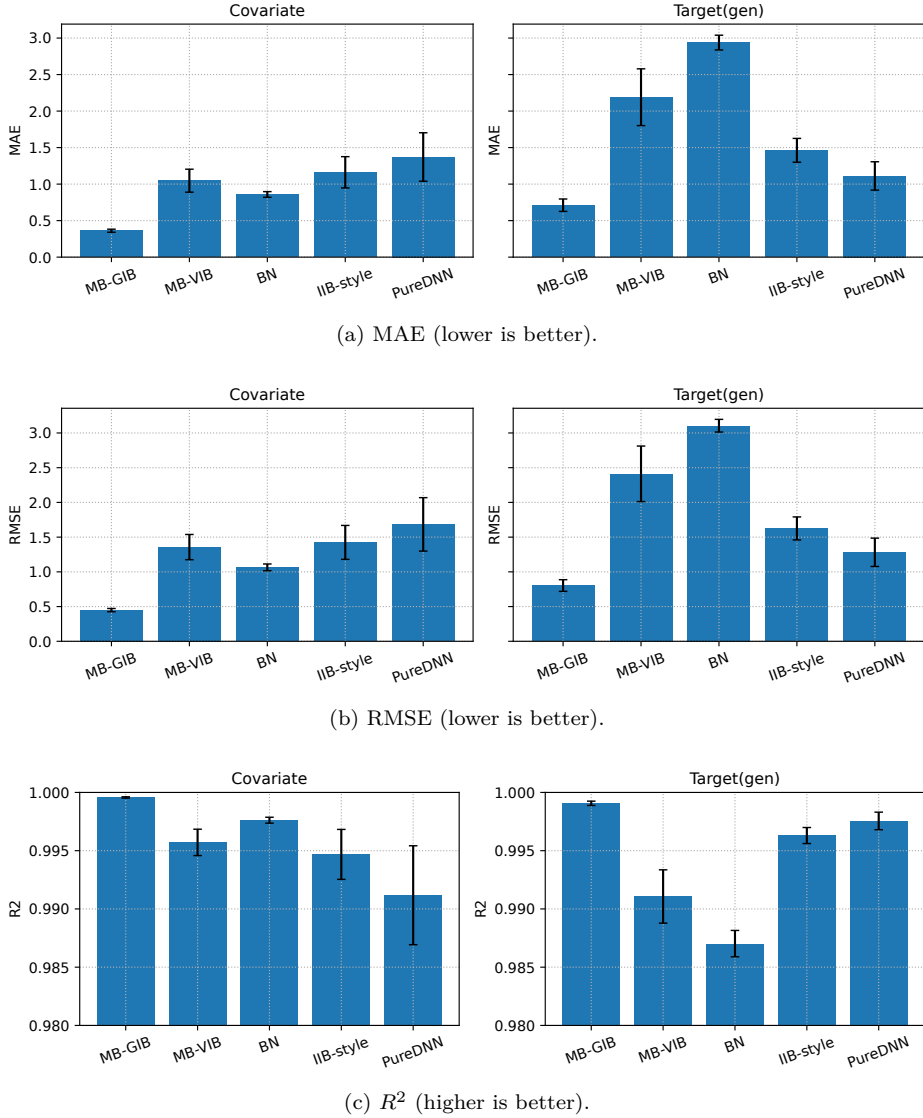


Figure 3: **Main comparison under covariate and generalized target shift.** Bars show mean \pm s.e. over seeds for MB-GIB, MB-VIB, BN, IIB-style, and pure DNN. MB-GIB dominates on all metrics; the gap is largest under target shift.

5.2 Simulated Experiments: MAGIC-IRRI Gene Network

We next consider a large-scale stress test on the 64-node *MAGIC-IRRI* Gaussian Bayesian network. To emulate strong experimental perturbations in a multi-trait genetic model, we apply three marginal-shift interventions on continuous covariates: **G4156** is shifted from $\mathcal{N}(0.7636, 0.9721^2)$ to $\mathcal{N}(1.5, 2.0^2)$, **G4573** from $\mathcal{N}(0.1196, 0.4744^2)$ to $\mathcal{N}(1.0, 1.0^2)$, and **G1533** from $\mathcal{N}(0.8004, 0.9803^2)$ to $\mathcal{N}(0, 3.0^2)$. After inducing these large shifts in the target domain, we hide the trait of interest HT and evaluate imputation from the remaining variables using several approaches: a source-trained Bayesian network (BN), mean/variance bottleneck variants (MB-GIB and MB-VIB), an IIB-style objective, and a pure feedforward DNN. All models are trained on the unshifted source and deployed zero-shot to the shifted domain.

Results and analysis. Table 2 shows that **MB-GIB** is the most accurate and robust method under simultaneous large marginal shifts, achieving the best MAE (5.57), RMSE (7.01), and $R^2 = 0.567$. **MB-VIB**

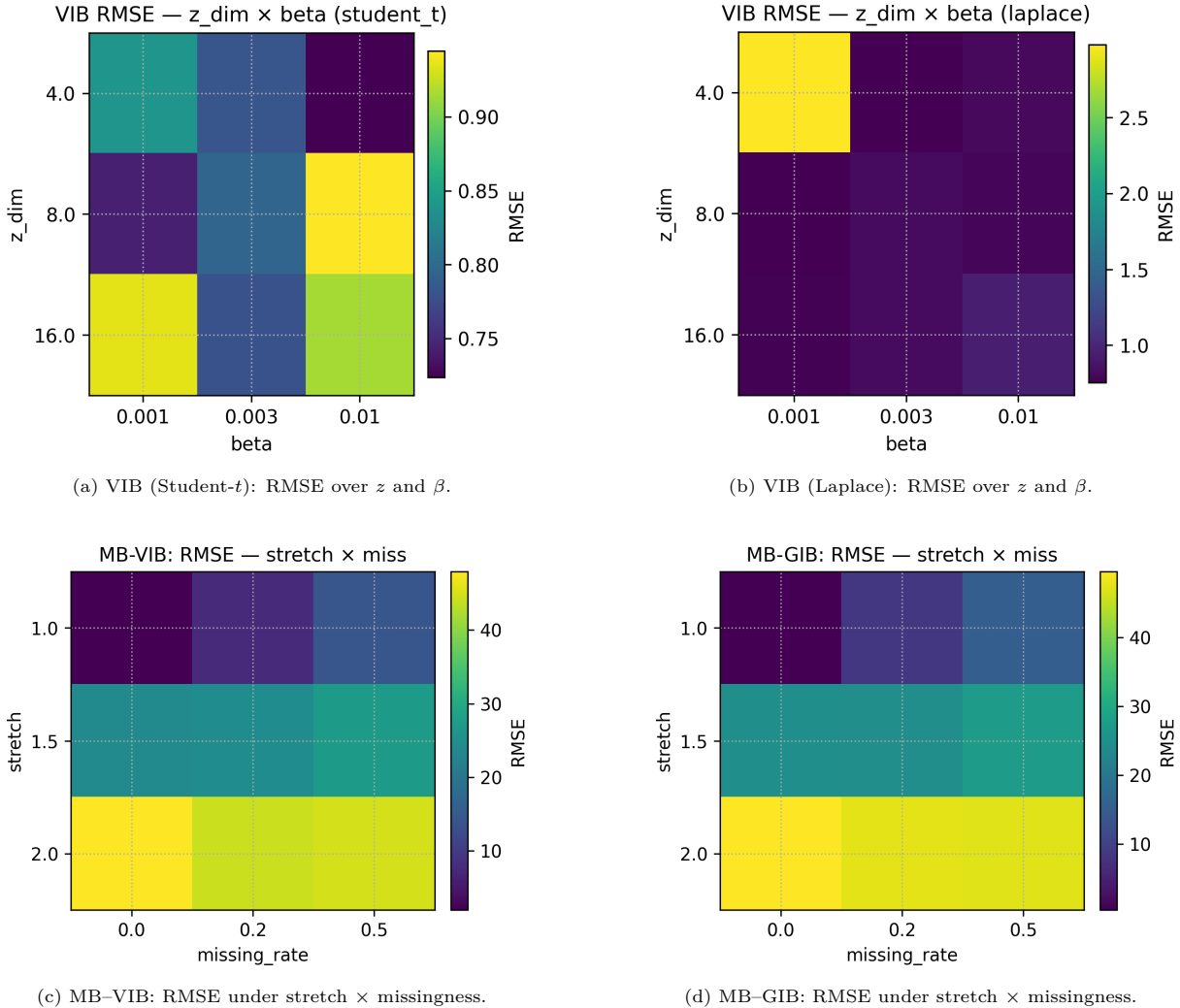


Figure 4: Heatmap summaries. **Top:** Ablation of VIB capacity (z) and compression (β) for two likelihoods. **Bottom:** Sensitivity to support mismatch (stretch) and missing rate for MB-VIB and MB-GIB. Lower is better (RMSE).

remains competitive but lags behind MB-GIB (MAE 7.08, RMSE 10.02, $R^2 = 0.121$), and the **IIB-style** variant performs similarly to MB-VIB. The source BN baseline degrades noticeably in this out-of-distribution regime (negative $R^2 = -0.096$), indicating that purely generative propagation without an information bottleneck is vulnerable to large marginal shifts. The **pure DNN** fails dramatically (MAE 14.45, RMSE 17.79, $R^2 = -1.77$), consistent with overfitting to source support and poor extrapolation. Overall, the results support the view that *compression with moment control* (as in MB-GIB) provides a better bias-variance tradeoff for zero-shot deployment under strong distribution shift in high-dimensional causal networks.

5.3 Real-Data Experiment on Single-Cell Signaling Networks

To assess performance in a setting with genuine biological heterogeneity, we use the seminal single-cell flow-cytometry compendium of Sachs *et al.* Sachs et al. (2005), which quantifies phosphorylation levels for a panel of signaling proteins in human primary CD4⁺ T cells subjected to controlled perturbations. The experimental conditions in this dataset create natural distributional shifts, providing a robust testbed for causal transfer. In our study, the anti-CD3/CD28 stimulation (853 cells) serves as the *source* domain, while

Table 2: Imputation performance on the MAGIC-IRRI DAG under multiple large-shift interventions.

Method	MAE	RMSE	R^2
Bayesian Network	9.3827	11.1872	-0.0957
MB-GIB	5.5706	7.0083	0.5670
MB-VIB	7.0837	10.0190	0.1211
IIB-style	7.8219	10.0456	0.1165
Pure DNN	14.4523	17.7908	-1.7711

the phorbol ester PMA condition (913 cells) is treated as the *target*. The latter directly activates PKC and reshapes downstream pathways in ways not present under CD3/CD28, yielding a demanding transfer scenario. With this split fixed, we evaluate models on imputing/forecasting the activities of ten key nodes in the pathway: Raf, Mek, Plcg, PIP₂, PIP₃, Erk, Akt, PKA, P38, and Jnk. Quantitative results—reported as mean absolute error (MAE), root mean squared error (RMSE), and coefficient of determination (R^2)—are summarized in Table 3.

Table 3: Imputation performance on the Sachs et al. data under multiple interventions.

Target	Method	MAE	RMSE	R^2	Target	Method	MAE	RMSE	R^2
Raf	Bayesian Network	0.6908	1.0015	-0.0041	Erk	Bayesian Network	0.5884	0.8379	0.2971
	MB-GIB	0.4132	0.6393	0.5908		MB-GIB	0.1817	0.2854	0.9184
	MB-VIB	0.4562	0.6821	0.5343		MB-VIB	0.3527	0.402	0.7691
	IIB-style	0.4422	0.6840	0.5316		IIB-style	0.424	0.5919	0.6496
	Pure DNN	0.5205	0.7815	0.3885		Pure DNN	0.3397	0.4499	0.7973
Mek	Bayesian Network	0.3935	0.6385	0.5919	Akt	Bayesian Network	0.1744	0.2756	0.9239
	MB-GIB	0.3935	0.6385	0.5919		MB-GIB	0.1744	0.2756	0.9239
	MB-VIB	0.4306	0.7032	0.5050		MB-VIB	0.2186	0.3014	0.9090
	IIB-style	0.5348	1.0905	-0.1904		IIB-style	0.3901	0.4595	0.7885
	Pure DNN	0.7599	1.2648	-0.6014		Pure DNN	0.2475	0.3505	0.8769
Plcg	Bayesian Network	0.6529	0.9995	-0.0000	PKA	Bayesian Network	0.6810	0.9992	0.0006
	MB-GIB	0.5858	0.9008	0.1876		MB-GIB	0.5114	0.7376	0.4552
	MB-VIB	0.5326	0.8075	0.3472		MB-VIB	1.6468	2.3798	-4.6698
	IIB-style	0.444	0.6999	0.5095		IIB-style	0.8304	1.5230	-1.3221
	Pure DNN	0.6443	1.0064	-0.0139		Pure DNN	1.0835	1.5752	-1.4842
PIP2	Bayesian Network	0.6156	0.8253	0.3179	P38	Bayesian Network	0.2896	0.4542	0.7934
	MB-GIB	0.6156	0.8254	0.3179		MB-GIB	0.2896	0.4542	0.7934
	MB-VIB	0.4976	0.7609	0.4203		MB-VIB	0.2801	0.4542	0.7934
	IIB-style	0.5158	0.9556	0.0856		IIB-style	0.3087	0.448	0.7647
	Pure DNN	0.4655	0.7948	0.3675		Pure DNN	0.2850	0.4609	0.7873
PIP3	Bayesian Network	0.5240	0.9280	0.1378	Jnk	Bayesian Network	0.6621	1.1185	-0.2525
	MB-GIB	0.3809	0.8106	0.3421		MB-GIB	0.6621	1.1185	-0.2525
	MB-VIB	0.3489	0.8307	0.3090		MB-VIB	0.6784	1.1327	-0.2844
	IIB-style	0.5336	1.2618	-0.5939		IIB-style	0.6784	1.1347	-0.2889
	Pure DNN	0.5219	1.3457	-0.8131		Pure DNN	0.7111	1.1530	-0.3310

Across the ten targets, bottleneck-based imputers are consistently strong under multiple interventions. In particular, MB-GIB attains the best or tied-best scores on *Raf*, *Erk*, and *PKA*, delivering large error reductions and high R^2 (e.g., $R^2=0.9184$ on *Erk*). MB-VIB is competitive—most notably it achieves the best RMSE and R^2 on *PIP2* and near-best on *PIP3*. IIB-style excels on *Plcg* where it achieves the top performance across all three metrics. By contrast, the Pure DNN lags on several targets and frequently yields negative R^2 , indicating overfitting or poor robustness to distribution shift induced by interventions.

The Bayesian Network (BN) remains a strong baseline on some nodes, tying for best on *Mek*, *Akt*, *P38*, and *Jnk*, suggesting that when local dependencies are simple or close to Gaussian/linear, a structured generative model can be sufficient. However, on targets where intervention-induced heterogeneity is more pronounced (*Raf*, *Erk*, *PKA*), mean-aware bottlenecking (MB-GIB) offers clear gains, pointing to better invariance and regularization under shift. Discrepancies between MAE and RMSE (e.g., *PIP2*) imply differing outlier sensitivity across methods; MB-VIB’s RMSE lead there suggests improved handling of rare but large errors. Overall, the results favor MB-GIB as the most reliable across interventions, with MB-VIB and IIB-style providing complementary strengths on specific targets, and BN serving as a competitive fallback where structure is well aligned with the data.

5.4 Extensions and Limitations

Extensions. The framework naturally accommodates (i) *partial or learned blankets*: estimate a candidate $MB(T)$ from local discovery around T and prune by conditional-independence tests; (ii) *parents-only* encoders when downstream paths are unstable; (iii) *multi-environment* training by sharing the decoder $q_\theta(t | z)$ across environments while allowing environment-specific encoders or priors; (iv) *semi-supervised* target settings with a small labeled subset to fine-tune the decoder; and (v) *uncertainty quantification* via the VIB decoder’s predictive variance/entropy and MB-GIB’s linear-Gaussian posterior formulas.

Limitations. Performance hinges on the *MB-invariance* assumption; mechanism drift in $p(T | X_M)$ (e.g., new parents of T , altered noise law) breaks zero-shot guarantees. Mis-specified or incomplete blankets (omitted true parents/spouses) can leak shift through $X \setminus M$ or reduce efficiency. Severe support shift in X_M induces extrapolation regardless of model class. VIB requires tuning (d_z, β) and sufficient data; over-capacity can overfit nuisance within M , while under-capacity can underfit $p(T | X_M)$. We recommend routine diagnostics: compare source vs. target decoder log-likelihoods and residuals of $\hat{g}(X_{M,t})$ to flag violations; if detected, shrink to parents-only, increase β (more compression), or incorporate limited target labels to recalibrate the decoder. *Finite-sample/optimization:* MB-GIB requires well-conditioned covariances; MB-VIB needs capacity control and early stopping. *Latent confounding:* Hidden parents of T that also affect X_M can violate conditional independence assumptions; instrumental/negative-control extensions are a promising avenue but beyond our scope.

6 Conclusion

We presented a *DAG-aware Information Bottleneck* for causal domain adaptation when the target variable is entirely missing at deployment. Our approach—MB-GIB in the linear-Gaussian regime and MB-VIB for nonlinear or non-Gaussian data—learns a compact, mechanism-stable summary confined to the Markov blanket of the target. Theoretically, we showed that in the Gaussian case the bottleneck reduces to CCA with a lossless restriction to the blanket, and that source-trained predictors transfer zero-shot under MB-invariance. Empirically, across a controlled 7-node SEM, the 64-node MAGIC-IRRI network, and a single-cell signaling dataset, the bottleneck family attains accurate imputations and remains robust under large covariate and generalized target shifts.

Beyond performance, the practical recipe is simple: (i) restrict encoders to parents or the Markov blanket, (ii) choose MB-GIB for fast, closed-form estimation or MB-VIB for flexible likelihoods, and (iii) deploy zero-shot to the target. Routine diagnostics (residual stability, likelihood checks) help detect violations of MB-invariance; when detected, shrinking to parents-only, increasing compression, or leveraging a small set of target labels restores reliability.

This work turns local causal knowledge into a lightweight, scalable toolkit for imputation under shift. Future directions include handling mechanism drift inside the blanket, learning blankets with uncertainty, incorporating instrumental/negative controls for latent confounding, and extending to multi-environment training with shared decoders and environment-specific encoders. We hope these results encourage broader use of mechanism-stable, bottlenecked representations as a practical bridge between causal structure and real-world domain adaptation.

References

Alessandro Achille and Stefano Soatto. Emergence of invariance and disentanglement in deep representations. *Journal of Machine Learning Research*, 19(50):1–34, 2018.

Alexander A Alemi, Ian Fischer, Joshua V Dillon, and Kevin Murphy. Deep variational information bottleneck. *arXiv preprint arXiv:1612.00410*, 2016.

Martin Arjovsky, Léon Bottou, Ishaaan Gulrajani, and David Lopez-Paz. Invariant risk minimization. *arXiv preprint arXiv:1907.02893*, 2019.

Elias Bareinboim and Judea Pearl. Transportability of causal effects: Completeness results. *UAI*, 2011.

Elias Bareinboim and Judea Pearl. Causal transportability with limited experiments. *AAAI*, 2012.

Elias Bareinboim and Judea Pearl. External validity: From do-calculus to transportability across populations. In *Journal of Causal Inference*, 2014.

Christopher P Burgess, Irina Higgins, Arka Pal, Loic Matthey, Nick Watters, Guillaume Desjardins, and Alexander Lerchner. Understanding disentangling in \beta-vae. *arXiv preprint arXiv:1804.03599*, 2018.

Gal Chechik, Amir Globerson, Naftali Tishby, and Yair Weiss. Information bottleneck for gaussian variables. *Advances in Neural Information Processing Systems*, 16, 2003.

Rodrigo Correa and Elias Bareinboim. Transportability of experimental results: A formal approach. In *IJCAI*, 2019.

Ian Fischer. The conditional entropy bottleneck. *Entropy*, 22(9):999, 2020.

Huan Hua, Jun Yan, Xi Fang, Weiquan Huang, Huilin Yin, and Wancheng Ge. Causal information bottleneck boosts adversarial robustness of deep neural network. *arXiv preprint arXiv:2210.14229*, 2022.

Fredrik D. Johansson, Uri Shalit, and David Sontag. Prediction under distribution shift: A causal perspective. In *NeurIPS*, 2019.

William M. Kouw and Marco Loog. A review of domain adaptation without target labels. *IEEE Trans. Pattern Analysis and Machine Intelligence*, 2019.

David Krueger, Vicent Cabannes, Ishmael Belghazi, Ben Poole, et al. Out-of-distribution generalization via risk extrapolation (rex). In *ICML*, 2021.

Bo Li, Yifei Shen, Yezhen Wang, Wenzhen Zhu, Dongsheng Li, Kurt Keutzer, and Han Zhao. Invariant information bottleneck for domain generalization. In *Proceedings of the AAAI Conference on Artificial Intelligence*, volume 36, pp. 7399–7407, 2022.

Zachary C. Lipton, Anima Wang, and Alex Smola. Detecting and correcting for label shift with black box predictors. In *ICML*, 2018.

Fangrui Lv, Jian Liang, Shuang Li, Bin Zang, Chi Harold Liu, Ziteng Wang, and Di Liu. Causality inspired representation learning for domain generalization. In *Proceedings of the IEEE/CVF conference on computer vision and pattern recognition*, pp. 8046–8056, 2022.

Luca Magliacane, Thomas Claassen, Karsten Borgwardt, and F. Dániel. Domain adaptation by using causal inference to predict invariant conditional distributions. In *NeurIPS*, 2018.

Judea Pearl. *Causality: Models, Reasoning, and Inference*. Cambridge University Press, 2009.

Jonas Peters, Peter Bühlmann, and Nicolai Meinshausen. Causal inference using invariant prediction: Identification and confidence intervals. In *JRSS-B*, 2016.

Nina Pfister, Peter Bühlmann, and Jonas Peters. Invariant causal prediction for sequential data: What if the markov assumption fails? In *AISTATS*, 2019a.

Nina Pfister, Peter Bühlmann, and Jonas Peters. Stabilizing causal structure learning via invariant conditional distributions. *Biometrika*, 2019b.

Ben Poole, Sherjil Ozair, Aaron Van Den Oord, Alex Alemi, and George Tucker. On variational bounds of mutual information. In *International conference on machine learning*, pp. 5171–5180. PMLR, 2019.

Ievgen Redko, Emilie Morvant, Amaury Habrard, Marc Sebban, and Younes Bennani. *Advances in domain adaptation theory*. Elsevier, 2019.

Marta Rojas-Carulla, Bernhard Schölkopf, Richard E. Turner, and Jonas Peters. Invariant models for causal transfer learning. In *JMLR Workshop and Conference Proceedings*, volume 63, pp. 752–760, 2018.

Karen Sachs, Omar Perez, Dana Pe’er, Douglas A Lauffenburger, and Garry P Nolan. Causal protein-signaling networks derived from multiparameter single-cell data. *Science*, 308(5721):523–529, 2005.

Hidekori Shimodaira. Improving predictive inference under covariate shift by weighting the log-likelihood function. *Journal of Statistical Planning and Inference*, 90:227–244, 2000.

Francisco N. F. Q. Simoes, Mehdi Dastani, and Thijs van Ommen. The causal information bottleneck and optimal causal variable abstractions. In *Proceedings of the 41st Conference on Uncertainty in Artificial Intelligence (UAI)*, 2025.

Noam Slonim and Naftali Tishby. Agglomerative information bottleneck. *Advances in neural information processing systems*, 12, 1999.

Noam Slonim, Nir Friedman, and Naftali Tishby. Agglomerative multivariate information bottleneck. *Advances in neural information processing systems*, 14, 2001.

Noam Slonim, Nir Friedman, and Naftali Tishby. Multivariate information bottleneck. *Neural computation*, 18(8):1739–1789, 2006.

Amos J. Storkey. When training and test sets are different: Characterizing learning transfer. In *Dataset Shift in Machine Learning*, 2009.

Daniel J Strouse and David J Schwab. The deterministic information bottleneck. *Neural computation*, 29(6):1611–1630, 2017.

Amit Subbaswamy and Suchi Saria. Preventing failure in exogenous distribution shift: A causal abstraction approach. In *NeurIPS*, 2018.

Amit Subbaswamy and Suchi Saria. Preventing failure under distribution shift using risk extrapolation. In *ICML*, 2019.

Masashi Sugiyama, Martin Krauledat, and Klaus-Robert Müller. Covariate shift adaptation by importance weighted cross validation. In *Journal of Machine Learning Research*, volume 8, pp. 985–1005. 2008.

Naftali Tishby and Noga Zaslavsky. Deep learning and the information bottleneck principle. In *2015 ieee information theory workshop (itw)*, pp. 1–5. Ieee, 2015.

Naftali Tishby, Fernando C Pereira, and William Bialek. The information bottleneck method. *arXiv preprint physics/0004057*, 2000.

Kaidi Zhang, Ding-Xuan Zhou, Rong Jin, and Bernhard Schölkopf. Domain adaptation under target and conditional shift. In *UAI*, 2013.

A Appendix: Theoretical Results and Proofs For main Claims in Sections 4.1 and 4.2

MB–GIB is Globally Optimal (Linear–Gaussian / CCA)

Claim. Under a linear–Gaussian structural equation model (SEM), *Markov-blanket GIB is globally optimal* for any bottleneck dimension d . The argument uses only Gaussian conditional independence and the CCA/GIB equivalence.

Block notation and MB identity. Partition $X = (M, N)$ and write

$$\Sigma_{XX} = \begin{bmatrix} \Sigma_{MM} & \Sigma_{MN} \\ \Sigma_{NM} & \Sigma_{NN} \end{bmatrix}, \quad \Sigma_{XT} = \begin{bmatrix} \Sigma_{MT} \\ \Sigma_{NT} \end{bmatrix}.$$

For Gaussians, $T \perp\!\!\!\perp N \mid M$ is equivalent to the vanishing conditional cross-covariance

$$\Sigma_{NT \cdot M} := \Sigma_{NT} - \Sigma_{NM} \Sigma_{MM}^{-1} \Sigma_{MT} = 0,$$

hence

$$\Sigma_{NT} = \Sigma_{NM} \Sigma_{MM}^{-1} \Sigma_{MT}. \quad (1)$$

Factorization of Σ_{XT} via M . Let

$$L := \begin{bmatrix} I_{|M|} \\ B \end{bmatrix}, \quad B := \Sigma_{NM} \Sigma_{MM}^{-1}.$$

Then equation 1 yields

$$\Sigma_{XT} = \begin{bmatrix} \Sigma_{MT} \\ \Sigma_{NT} \end{bmatrix} = \begin{bmatrix} I \\ B \end{bmatrix} \Sigma_{MT} = L \Sigma_{MT}. \quad (2)$$

CCA operators and a key metric identity. Define the (symmetric) CCA/IB operators

$$\Omega_X := \Sigma_{XX}^{-1/2} \Sigma_{XT} \Sigma_{TT}^{-1} \Sigma_{TX} \Sigma_{XX}^{-1/2}, \quad \Omega_M := \Sigma_{MM}^{-1/2} \Sigma_{MT} \Sigma_{TT}^{-1} \Sigma_{TM} \Sigma_{MM}^{-1/2}.$$

Using equation 2,

$$\Omega_X = (\Sigma_{XX}^{-1/2} L) \underbrace{(\Sigma_{MT} \Sigma_{TT}^{-1} \Sigma_{TM})}_{=:K} (\Sigma_{XX}^{-1/2} L)^\top.$$

A standard block-inverse (Schur-complement) calculation under $\Sigma_{NT \cdot M} = 0$ gives the metric identity

$$L^\top \Sigma_{XX}^{-1} L = \Sigma_{MM}^{-1}. \quad (3)$$

Equivalently,

$$\Sigma_{XX}^{-1/2} L = Q \Sigma_{MM}^{-1/2} \quad \text{for some column-orthonormal } Q \quad (Q^\top Q = I_{|M|}).$$

Same canonical correlations via SVD. Let

$$S_X := \Sigma_{XX}^{-1/2} \Sigma_{XT} \Sigma_{TT}^{-1/2} = (\Sigma_{XX}^{-1/2} L) (\Sigma_{MT} \Sigma_{TT}^{-1/2}) = Q \underbrace{(\Sigma_{MM}^{-1/2} \Sigma_{MT} \Sigma_{TT}^{-1/2})}_{=:S_M}.$$

Since Q has orthonormal columns, left-multiplication by Q preserves singular values, hence

$$\text{singvals}(S_X) = \text{singvals}(S_M).$$

Therefore the canonical correlations for (X, T) equal those for (M, T) , and the nonzero spectra of $\Omega_X = S_X S_X^\top$ and $\Omega_M = S_M S_M^\top$ coincide.

Range containment and lifted eigenvectors. From the factorization,

$$\text{range}(\Omega_X) \subseteq \text{range}(\Sigma_{XX}^{-1/2} L) = \text{range}(Q \Sigma_{MM}^{-1/2}) = \left\{ \Sigma_{XX}^{-1/2} \begin{bmatrix} u \\ Bu \end{bmatrix} : u \in \mathbb{R}^{|M|} \right\}.$$

If v_M is an eigenvector of Ω_M with a nonzero eigenvalue, then $v_X := Q v_M$ is an eigenvector of Ω_X with the same eigenvalue.

Equivalence of optimal d -dimensional subspaces. Let $\mathcal{S}_d(X)$ and $\mathcal{S}_d(M)$ be any optimal d -dimensional IB/CCA subspaces. Then

$$\mathcal{S}_d(X) = \Sigma_{XX}^{-1/2} L \Sigma_{MM}^{1/2} \mathcal{S}_d(M) = Q \mathcal{S}_d(M),$$

i.e., the optimal X -subspace is exactly the *isometric lift* of the optimal M -subspace. Hence restricting IB/CCA to the Markov blanket M incurs no loss for any d .

Remark on prediction risk. Since $\Sigma_{XT} = L \Sigma_{MT}$ and $L = [I; B]$, we have $\mathbb{E}[T \mid X] = \mathbb{E}[T \mid M]$ (the Schur-complement condition $\Sigma_{NT \cdot M} = 0$). Thus the Bayes MSE using X equals that using M ; the IB-optimal linear summaries agree up to the isometry Q .

Justifying MB–VIB Beyond Gaussianity

You can justify *MB–VIB* (using only the Markov blanket of T) well beyond Gaussianity with information-theoretic and causal arguments that do not depend on linearity or normality.

1) Information-theoretic sufficiency (distribution-free)

Let $X = (M, N)$ where $M := \text{MB}(T)$ and $N := X \setminus M$. In any DAG-Markov distribution (not necessarily Gaussian),

$$T \perp\!\!\!\perp N \mid M.$$

Then:

- All predictive information is in M :

$$I(T; X) = I(T; (M, N)) = I(T; M) + I(T; N \mid M) = I(T; M),$$

since $I(T; N \mid M) = 0$ by conditional independence.

- **IB objective cannot benefit from N :** The (variational) IB Lagrangian for any representation $U = f(X)$ is

$$\mathcal{L}_\beta(f) = I(X; U) - \beta I(T; U).$$

By the data processing inequality (DPI),

$$I(T; U) \leq I(T; X) = I(T; M).$$

Moreover, any U that is a function of M can achieve the same upper bound on $I(T; U)$ as any U that also sees N (since N contains no extra information about T given M). But using N can only *increase* the compression cost $I(X; U)$ (the encoder ingests more input), so among encoders with the same $I(T; U)$, those depending only on M weakly *dominate* in \mathcal{L}_β .

Population-level proposition (no Gaussianity). If $T \perp\!\!\!\perp N \mid M$ and the encoder class is rich enough to approximate measurable functions, then for every $\beta > 0$ there exists an IB-optimal encoder f^* that depends only on M . Equivalently, restricting IB to M does not worsen the optimal IB value.

Sketch. For any encoder $f(M, N)$, define $g(M) = \mathbb{E}[f(M, N) \mid M]$ or a sufficient surrogate achieving the same $I(T; U)$. By DPI and $T \perp\!\!\!\perp N \mid M$, the value $I(T; g(M)) \geq I(T; f(M, N))$ is achievable, while $I(X; g(M)) \leq I(X; f(M, N))$. Hence $\mathcal{L}_\beta(g) \leq \mathcal{L}_\beta(f)$.

2) Predictive optimality via conditional sufficiency

Independently of IB, the Bayes predictor satisfies

$$p(T | X) = p(T | M),$$

so the *minimal sufficient statistic* for predicting T is any representation that preserves $p(T | M)$. Thus, if the VIB encoder/decoder can approximate $p(T | U)$, then any VIB-optimal representation can be chosen to be a function of M ; including N brings no improvement to (population) predictive risk.

3) Robustness to shift and interventions (causal justification)

- Under *covariate shift* where $p(X)$ changes but the mechanism $p(T | \text{pa}(T))$ stays fixed, non-blanket variables N can drift via $p(N | M)$ without changing $p(T | M)$. Using N risks encoding unstable directions; restricting to M preserves the invariant conditional.
- Under *soft interventions* on variables outside $\text{MB}(T)$, $p(T | M)$ remains invariant by the causal Markov property, while $p(T | X)$ (if it exploits N) can change. MB–VIB therefore targets invariant predictive structure.

4) Beyond linear/Gaussian encoders (practical learnability)

- With nonlinear VIB (neural encoders/decoders), universal approximation allows a representation $U = \phi(M)$ that is (approximately) sufficient for T without using N . This holds for non-Gaussian and nonlinear SEMs so long as $T \perp\!\!\!\perp N | M$.
- With finite samples and model/regularization constraints, MB–VIB often helps by reducing variance and avoiding spurious correlations—another reason it can outperform global inputs under shift.

5) When MB–VIB might not be optimal

- If the Markov blanket is *misspecified* (e.g., hidden confounders or measurement error breaking $T \perp\!\!\!\perp N | M$), some components of N may carry residual predictive information; global representations can help.
- If only a *subset* of M is observed (missing parents/children/spouses), certain N variables may act as proxies; the MB restriction could be too strict.
- With a *tight* encoder class (very low capacity or heavy regularization), allowing N might accidentally aid approximation—even though it adds no information in principle.

Bottom line (distribution-free)

1. **Sufficiency:** $T \perp\!\!\!\perp N | M \Rightarrow I(T; X) = I(T; M)$ and $p(T | X) = p(T | M)$.
2. **IB dominance:** For the IB objective $I(X; U) - \beta I(T; U)$, any benefit to $I(T; U)$ achievable with X is achievable with M alone, while $I(X; U)$ cannot be smaller when using superfluous inputs.
3. **Invariance:** MB focuses the encoder on causally relevant mechanisms, the ones most likely to remain stable across domains.

None of these require Gaussianity or linearity; they rely only on conditional independence and data processing / information sufficiency.

In this context, **whitening** means linearly transforming a zero-mean vector so its covariance becomes the identity. If $X \in \mathbb{R}^q$ has mean μ_X and covariance $\Sigma_{XX} \succ 0$, a (symmetric) whitener is $\Sigma_{XX}^{-1/2}$ (from an eigendecomposition or Cholesky). The whitened variable is

$$\tilde{X} = \Sigma_{XX}^{-1/2}, (X - \mu_X), \quad \text{Cov}(\tilde{X}) = I_q.$$

Intuitively, whitening de-correlates the coordinates and rescales each to unit variance.

B Appendix: Theoretical Results and Proofs For main Claims in Section 4.4

Proof of Theorem 1. Let $d := p + 1$ and let $Z_1, \dots, Z_n \in \mathbb{R}^d$ be i.i.d. copies of $Z = (X_M^\top, T)^\top$ with $\mathbb{E}(Z) = 0$ and covariance $\Sigma = \text{Cov}(Z) = \mathbb{E}[ZZ^\top]$. For simplicity, define the uncentered second-moment estimator

$$\widehat{\Sigma} := \frac{1}{n} \sum_{i=1}^n Z_i Z_i^\top.$$

The centered sample covariance $\widehat{\Sigma}_c := \frac{1}{n} \sum_{i=1}^n (Z_i - \bar{Z})(Z_i - \bar{Z})^\top$ satisfies $\widehat{\Sigma}_c = \widehat{\Sigma} - \bar{Z}\bar{Z}^\top$. Moreover, $\|\bar{Z}\bar{Z}^\top\|_{\text{op}} = \|\bar{Z}\|_2^2$ and a standard sub-Gaussian mean bound yields $\|\bar{Z}\|_2 \leq CK \left(\sqrt{\frac{d+\log(1/\delta)}{n}} + \frac{d+\log(1/\delta)}{n} \right)$ with probability at least $1 - \delta$, hence $\|\bar{Z}\bar{Z}^\top\|_{\text{op}} \leq C'K^2 \frac{d+\log(1/\delta)}{n}$. This term is dominated by the stated rate, so the same bound holds for $\widehat{\Sigma}_c$ up to constants.

Under Assumption 1, the random vector Z is K -sub-Gaussian. A standard non-asymptotic covariance estimation theorem for general (non-isotropic) sub-Gaussian vectors (e.g., Vershynin, *High-Dimensional Probability*, 2018, covariance estimation for sub-Gaussian vectors; see Theorem 4.7.1 in the Cambridge edition) implies that for any $\delta \in (0, 1)$, with probability at least $1 - \delta$,

$$\|\widehat{\Sigma} - \Sigma\|_{\text{op}} \leq cK^2 \left(\sqrt{\frac{d + \log(1/\delta)}{n}} + \frac{d + \log(1/\delta)}{n} \right),$$

for a universal constant $c > 0$. Substituting $d = p + 1$ yields the stated bound.

Finally, the same high-probability bound holds for each covariance block. For any principal block B of a symmetric matrix A , $\|B\|_{\text{op}} \leq \|A\|_{\text{op}}$. For the cross-covariance block, partitioning indices by (X_M, T) , we have

$$\|A_{X_M T}\|_{\text{op}} = \sup_{\|u\|_2 = \|v\|_2 = 1} u^\top A_{X_M T} v = \sup_{\|u\|_2 = \|v\|_2 = 1} \tilde{u}^\top A \tilde{v} \leq \|A\|_{\text{op}},$$

where $\tilde{u} = (u^\top, 0)^\top$ and $\tilde{v} = (0, v)^\top$ are unit vectors in \mathbb{R}^d and $u \in \mathbb{R}^p$ and $v \in \mathbb{R}$ since T is scalar.

Applying this to $A = \widehat{\Sigma} - \Sigma$ completes the proof. \square

Proof of Theorem 2. Recall

$$\Omega_M = \Sigma_{XX}^{-1/2} \Sigma_{XT} \Sigma_{TT}^{-1} \Sigma_{TX} \Sigma_{XX}^{-1/2}, \quad \widehat{\Omega}_M = \widehat{\Sigma}_{XX}^{-1/2} \widehat{\Sigma}_{XT} \widehat{\Sigma}_{TT}^{-1} \widehat{\Sigma}_{TX} \widehat{\Sigma}_{XX}^{-1/2}.$$

Throughout this proof, we abbreviate $\Sigma_{X_M X_M}$ as Σ_{XX} for notational simplicity, with the understanding that this refers to the Markov blanket covariance. Also, we use the partition $Z = (X_M^\top, T)^\top$, so $\Sigma_{TT} \in \mathbb{R}$ is a scalar variance. Since T is one-dimensional, we may (and do) assume w.l.o.g. that $\Sigma_{TT} = 1$ by rescaling T ; this only rescales K and does not affect the form of the rate.

Step 1: Davis–Kahan for symmetric eigen-subspaces. Both Ω_M and $\widehat{\Omega}_M$ are symmetric positive semidefinite. Let $\lambda_1 \geq \dots \geq \lambda_p$ be the eigenvalues of Ω_M and assume the eigengap $\gamma = \lambda_d - \lambda_{d+1} > 0$ (Assumption 3). The Davis–Kahan sin Θ theorem (in operator norm form) yields

$$\|\sin \Theta(\widehat{U}, U_\star)\|_{\text{op}} \leq \frac{C}{\gamma} \|\widehat{\Omega}_M - \Omega_M\|_{\text{op}}, \tag{4}$$

for a universal constant $C > 0$. Moreover, the projector bound $\|\widehat{\Pi} - \Pi_\star\|_{\text{op}} \leq 2\|\sin \Theta(\widehat{U}, U_\star)\|_{\text{op}}$ is standard.

Step 2: Reduce $\|\widehat{\Omega}_M - \Omega_M\|_{\text{op}}$ to covariance errors. Write

$$S := \Sigma_{XX}^{-1/2}, \quad \widehat{S} := \widehat{\Sigma}_{XX}^{-1/2}, \quad M := \Sigma_{XT} \Sigma_{TT}^{-1} \Sigma_{TX} = \Sigma_{XT} \Sigma_{TX}, \quad \widehat{M} := \widehat{\Sigma}_{XT} \widehat{\Sigma}_{TT}^{-1} \widehat{\Sigma}_{TX}.$$

Then $\Omega_M = SMS$ and $\widehat{\Omega}_M = \widehat{S} \widehat{M} \widehat{S}$, so

$$\widehat{\Omega}_M - \Omega_M = (\widehat{S} - S)\widehat{M}\widehat{S} + S(\widehat{M} - M)\widehat{S} + SM(\widehat{S} - S). \quad (5)$$

We work on the event

$$\mathcal{E} := \left\{ \|\widehat{\Sigma} - \Sigma\|_{\text{op}} \leq \frac{\lambda_0}{2} \right\} \cap \left\{ |\widehat{\Sigma}_{TT} - \Sigma_{TT}| \leq \frac{1}{2}\Sigma_{TT} \right\}, \quad (6)$$

which holds with probability at least $1 - \delta$ for suitable constants by Theorem 1 (applied with a union bound to the relevant blocks). On \mathcal{E} ,

$$\lambda_{\min}(\widehat{\Sigma}_{XX}) \geq \lambda_0/2, \quad \lambda_{\max}(\widehat{\Sigma}_{XX}) \leq \Lambda_0 + \lambda_0/2, \quad \widehat{\Sigma}_{TT} \in [1/2, 3/2].$$

Hence

$$\|S\|_{\text{op}} \leq \lambda_0^{-1/2}, \quad \|\widehat{S}\|_{\text{op}} \leq (\lambda_0/2)^{-1/2} = \sqrt{2}\lambda_0^{-1/2}. \quad (7)$$

Step 3: Control M, \widehat{M} and their perturbation. Since the full covariance matrix of (X_M, T) is positive semidefinite, its Schur complement implies

$$\Sigma_{XX} - \Sigma_{XT}\Sigma_{TT}^{-1}\Sigma_{TX} = \Sigma_{XX} - M \succeq 0,$$

so $0 \preceq M \preceq \Sigma_{XX}$ and therefore

$$\|M\|_{\text{op}} \leq \|\Sigma_{XX}\|_{\text{op}} \leq \Lambda_0. \quad (8)$$

Similarly, on \mathcal{E} , the empirical covariance is also positive semidefinite, giving $0 \preceq \widehat{M} \preceq \widehat{\Sigma}_{XX}$ (up to the scalar factor $\widehat{\Sigma}_{TT}^{-1} \in [2/3, 2]$), and thus

$$\|\widehat{M}\|_{\text{op}} \leq 2\|\widehat{\Sigma}_{XX}\|_{\text{op}} \leq 2(\Lambda_0 + \lambda_0/2) \leq 3\Lambda_0 \quad (\text{w.l.o.g. taking } \Lambda_0 \geq \lambda_0). \quad (9)$$

Next, bound $\|\widehat{M} - M\|_{\text{op}}$. Using $\Sigma_{TT} = 1$ and adding/subtracting terms,

$$\widehat{M} - M = (\widehat{\Sigma}_{XT} - \Sigma_{XT})\Sigma_{TX} + \widehat{\Sigma}_{XT}(\widehat{\Sigma}_{TT}^{-1} - 1)\Sigma_{TX} + \widehat{\Sigma}_{XT}\widehat{\Sigma}_{TT}^{-1}(\widehat{\Sigma}_{TX} - \Sigma_{TX}).$$

Each covariance block deviation is bounded by $\|\widehat{\Sigma} - \Sigma\|_{\text{op}}$ (as shown in the block argument in Theorem 1). Also, from $M \preceq \Sigma_{XX}$ we have $\|\Sigma_{XT}\|_{\text{op}}^2 = \|\Sigma_{XT}\Sigma_{TX}\|_{\text{op}} = \|M\|_{\text{op}} \leq \Lambda_0$, so $\|\Sigma_{XT}\|_{\text{op}} \leq \sqrt{\Lambda_0}$; the same reasoning on \mathcal{E} gives $\|\widehat{\Sigma}_{XT}\|_{\text{op}} \leq \sqrt{3\Lambda_0}$. Finally, on \mathcal{E} , $|\widehat{\Sigma}_{TT}^{-1} - 1| \leq 2|\widehat{\Sigma}_{TT} - 1| \leq 2\|\widehat{\Sigma} - \Sigma\|_{\text{op}}$. Putting these together yields, on \mathcal{E} ,

$$\|\widehat{M} - M\|_{\text{op}} \leq C_M \|\widehat{\Sigma} - \Sigma\|_{\text{op}}, \quad (10)$$

for a constant $C_M > 0$ depending only on Λ_0 (and the fixed variance normalization of T).

Step 4: Lipschitz bound for inverse square-roots. On \mathcal{E} , both Σ_{XX} and $\widehat{\Sigma}_{XX}$ have eigenvalues bounded below by $\lambda_0/2$. The matrix function $A \mapsto A^{-1/2}$ is operator-Lipschitz on $[\lambda_0/2, \infty)$, implying

$$\|\widehat{S} - S\|_{\text{op}} = \|\widehat{\Sigma}_{XX}^{-1/2} - \Sigma_{XX}^{-1/2}\|_{\text{op}} \leq C_S \|\widehat{\Sigma}_{XX} - \Sigma_{XX}\|_{\text{op}} \leq C_S \|\widehat{\Sigma} - \Sigma\|_{\text{op}}, \quad (11)$$

where $C_S > 0$ depends only on λ_0 (e.g., one may take $C_S \asymp \lambda_0^{-3/2}$).

Step 5: Bound $\|\widehat{\Omega}_M - \Omega_M\|_{\text{op}}$. Apply equation 5 and submultiplicativity, using equation 7, equation 8, equation 9, equation 10, and equation 11. On \mathcal{E} ,

$$\|\widehat{\Omega}_M - \Omega_M\|_{\text{op}} \leq \|\widehat{S} - S\|_{\text{op}} \|\widehat{M}\|_{\text{op}} \|\widehat{S}\|_{\text{op}} + \|S\|_{\text{op}} \|\widehat{M} - M\|_{\text{op}} \|\widehat{S}\|_{\text{op}} + \|S\|_{\text{op}} \|M\|_{\text{op}} \|\widehat{S} - S\|_{\text{op}} \leq C' \|\widehat{\Sigma} - \Sigma\|_{\text{op}},$$

for a constant $C' > 0$ depending only on λ_0, Λ_0 . This proves the second inequality in the theorem statement.

Step 6: Conclude and plug concentration. Combining equation 4 with the previous display gives, on \mathcal{E} ,

$$\|\sin \Theta(\widehat{U}, U_\star)\|_{\text{op}} \leq \frac{C}{\gamma} \|\widehat{\Omega}_M - \Omega_M\|_{\text{op}} \leq \frac{CC'}{\gamma} \|\widehat{\Sigma} - \Sigma\|_{\text{op}}.$$

Finally, Theorem 1 yields $\|\widehat{\Sigma} - \Sigma\|_{\text{op}} \lesssim K^2(\sqrt{(p + \log(1/\delta))/n} + (p + \log(1/\delta))/n)$, and for the usual regime $n \gtrsim p + \log(1/\delta)$ this implies the stated $\lesssim \frac{K^2}{\gamma} \sqrt{\frac{p + \log(1/\delta)}{n}}$ rate (absorbing constants into \lesssim). The projector inequality $\|\widehat{\Pi} - \Pi_\star\|_{\text{op}} \leq 2\|\sin \Theta(\widehat{U}, U_\star)\|_{\text{op}}$ follows from standard principal-angle identities. \square

Proof of Theorem 3. Write $X := X_M \in \mathbb{R}^p$. Under the Gaussian IB setting of Sec. 4.1 (jointly Gaussian (X, T)), the population conditional mean is linear:

$$g^*(x) = \mathbb{E}[T \mid X = x] = \beta^\top x, \quad \beta := \Sigma_{XX}^{-1} \Sigma_{XT},$$

(where we use $\mathbb{E}(Z) = 0$). Since T is one-dimensional, the CCA/GIB operator Ω_M has rank at most 1, and the MB–GIB encoder/decoder produces the same predictor as ordinary least squares on (X, T) (up to an irrelevant scaling of the latent). In particular, the empirical MB–GIB predictor \widehat{g} is of the form

$$\widehat{g}(x) = \widehat{\beta}^\top x, \quad \widehat{\beta} := \widehat{\Sigma}_{XX}^{-1} \widehat{\Sigma}_{XT},$$

where $\widehat{\Sigma}$ is the empirical covariance of $Z = (X^\top, T)^\top$ and $\widehat{\Sigma}_{XX}, \widehat{\Sigma}_{XT}$ are its blocks. (Equivalently: the top eigenvector of $\widehat{\Omega}_M$ is proportional to $\widehat{\Sigma}_{XX}^{-1/2} \widehat{\Sigma}_{XT}$; unwhitening yields $\widehat{W} \propto \widehat{\Sigma}_{XX}^{-1} \widehat{\Sigma}_{XT}$; the optimal linear decoder cancels the scaling.)

Step 1: Excess risk equals L_2 prediction error. For squared loss, the Bayes rule g^* is the conditional mean, and the excess risk satisfies the identity

$$\mathcal{R}_s(\widehat{g}) - \mathcal{R}_s(g^*) = \mathbb{E}[(\widehat{g}(X) - g^*(X))^2] = \mathbb{E}[(\widehat{\beta} - \beta)^\top X]^2 = (\widehat{\beta} - \beta)^\top \Sigma_{XX} (\widehat{\beta} - \beta).$$

Using Assumption 2, $\|\Sigma_{XX}\|_{\text{op}} \leq \Lambda_0$, hence

$$\mathcal{R}_s(\widehat{g}) - \mathcal{R}_s(g^*) \leq \Lambda_0 \|\widehat{\beta} - \beta\|_2^2. \quad (12)$$

Step 2: Lipschitz control of $\widehat{\beta}$ in terms of covariance errors. Let $\Delta_{XX} := \widehat{\Sigma}_{XX} - \Sigma_{XX}$ and $\Delta_{XT} := \widehat{\Sigma}_{XT} - \Sigma_{XT}$. Then

$$\widehat{\beta} - \beta = \widehat{\Sigma}_{XX}^{-1} \widehat{\Sigma}_{XT} - \Sigma_{XX}^{-1} \Sigma_{XT} = \widehat{\Sigma}_{XX}^{-1} \Delta_{XT} + (\widehat{\Sigma}_{XX}^{-1} - \Sigma_{XX}^{-1}) \Sigma_{XT}.$$

Work on the event

$$\mathcal{E} := \left\{ \|\widehat{\Sigma} - \Sigma\|_{\text{op}} \leq \frac{\lambda_0}{2} \right\}.$$

On \mathcal{E} , $\lambda_{\min}(\widehat{\Sigma}_{XX}) \geq \lambda_0/2$, hence

$$\|\widehat{\Sigma}_{XX}^{-1}\|_{\text{op}} \leq \frac{2}{\lambda_0}, \quad \|\Sigma_{XX}^{-1}\|_{\text{op}} \leq \frac{1}{\lambda_0}, \quad \|\widehat{\Sigma}_{XX}^{-1} - \Sigma_{XX}^{-1}\|_{\text{op}} \leq \|\widehat{\Sigma}_{XX}^{-1}\|_{\text{op}} \|\Delta_{XX}\|_{\text{op}} \|\Sigma_{XX}^{-1}\|_{\text{op}} \leq \frac{2}{\lambda_0^2} \|\Delta_{XX}\|_{\text{op}}.$$

Moreover, $\|\Delta_{XX}\|_{\text{op}} \leq \|\widehat{\Sigma} - \Sigma\|_{\text{op}}$ and $\|\Delta_{XT}\|_{\text{op}} \leq \|\widehat{\Sigma} - \Sigma\|_{\text{op}}$ by the block-operator bound used in Theorem 1. Finally, since the block covariance $\begin{pmatrix} \Sigma_{XX} & \Sigma_{XT} \\ \Sigma_{TX} & \Sigma_{TT} \end{pmatrix} \succeq 0$, its Schur complement gives $\Sigma_{XT} \Sigma_{TT}^{-1} \Sigma_{TX} \preceq \Sigma_{XX}$. Rescaling T so that $\Sigma_{TT} = 1$ (w.l.o.g. for a scalar T , absorbing this into K), we obtain $\|\Sigma_{XT}\|_{\text{op}}^2 = \|\Sigma_{XT} \Sigma_{TX}\|_{\text{op}} \leq \|\Sigma_{XX}\|_{\text{op}} \leq \Lambda_0$, hence $\|\Sigma_{XT}\|_{\text{op}} \leq \sqrt{\Lambda_0}$. Combining the above, on \mathcal{E} ,

$$\|\widehat{\beta} - \beta\|_2 \leq \|\widehat{\Sigma}_{XX}^{-1}\|_{\text{op}} \|\Delta_{XT}\|_{\text{op}} + \|\widehat{\Sigma}_{XX}^{-1} - \Sigma_{XX}^{-1}\|_{\text{op}} \|\Sigma_{XT}\|_{\text{op}} \leq \left(\frac{2}{\lambda_0} + \frac{2\sqrt{\Lambda_0}}{\lambda_0^2} \right) \|\widehat{\Sigma} - \Sigma\|_{\text{op}}.$$

Therefore,

$$\|\widehat{\beta} - \beta\|_2^2 \leq C_\beta \|\widehat{\Sigma} - \Sigma\|_{\text{op}}^2, \quad C_\beta := \left(\frac{2}{\lambda_0} + \frac{2\sqrt{\Lambda_0}}{\lambda_0^2} \right)^2, \quad (13)$$

where C_β depends only on λ_0, Λ_0 .

Step 3: Conclude the operator-norm-squared bound. Plugging equation 13 into equation 12 yields, on \mathcal{E} ,

$$\mathcal{R}_s(\widehat{g}) - \mathcal{R}_s(g^*) \leq \Lambda_0 C_\beta \|\widehat{\Sigma} - \Sigma\|_{\text{op}}^2 = C'' \|\widehat{\Sigma} - \Sigma\|_{\text{op}}^2,$$

with $C'' := \Lambda_0 C_\beta$, depending only on λ_0, Λ_0 , as claimed.

Step 4: Convert to an explicit rate via covariance concentration. By Theorem 1, with probability at least $1 - \delta$,

$$\|\widehat{\Sigma} - \Sigma\|_{\text{op}} \lesssim K^2 \left(\sqrt{\frac{p+1+\log(1/\delta)}{n}} + \frac{p+1+\log(1/\delta)}{n} \right).$$

Squaring and using the usual regime $n \gtrsim p + \log(1/\delta)$ gives

$$\mathcal{R}_s(\widehat{g}) - \mathcal{R}_s(g^*) \lesssim K^4 \frac{p + \log(1/\delta)}{n},$$

after absorbing constants into \lesssim . This completes the proof. \square

Proof of Corollary 1. For squared loss $\ell(t, \hat{t}) = (t - \hat{t})^2$, the Bayes rule is the conditional mean. Under MB invariance $p_s(T | X_M) = p_t(T | X_M)$, the conditional mean is shared: $g^*(x_M) = \mathbb{E}_{p_s}[T | X_M = x_M] = \mathbb{E}_{p_t}[T | X_M = x_M]$, and is target-optimal among predictors measurable w.r.t. X_M .

For any domain $\nu \in \{\text{s}, \text{t}\}$, the regression decomposition yields

$$\mathcal{R}_\nu(\widehat{g}) - \mathcal{R}_\nu(g^*) = \mathbb{E}_{p_\nu(X_M)}[(\widehat{g}(X_M) - g^*(X_M))^2],$$

which proves the stated conditional excess-risk identity.

If $p_t \ll p_s$ on X_M , then by change of measure,

$$\mathcal{R}_t(\widehat{g}) - \mathcal{R}_t(g^*) = \mathbb{E}_{p_s(X_M)} \left[(\widehat{g}(X_M) - g^*(X_M))^2 \frac{p_t(X_M)}{p_s(X_M)} \right] \leq \left(\text{ess sup}_{x_M} \frac{p_t(x_M)}{p_s(x_M)} \right) \mathbb{E}_{p_s(X_M)}[(\widehat{g}(X_M) - g^*(X_M))^2].$$

The last expectation equals $\mathcal{R}_s(\widehat{g}) - \mathcal{R}_s(g^*)$ by the same decomposition, yielding

$$\mathcal{R}_t(\widehat{g}) - \mathcal{R}_t(g^*) \leq \rho_M (\mathcal{R}_s(\widehat{g}) - \mathcal{R}_s(g^*)), \quad \rho_M := \text{ess sup}_{x_M} \frac{p_t(x_M)}{p_s(x_M)}.$$

Finally, applying Theorem 3 gives, with probability at least $1 - \delta$,

$$\mathcal{R}_t(\widehat{g}) - \mathcal{R}_t(g^*) \lesssim \rho_M K^4 \frac{p + \log(1/\delta)}{n}.$$

If $p_s(X_M) = p_t(X_M)$, then $\rho_M = 1$ and the source and target excess risks coincide. \square

Proof of Corollary 2. For squared loss, the regression decomposition implies that for any domain $\nu \in \{\text{s}, \text{t}\}$ and any predictor g ,

$$\mathcal{R}_\nu(g) - \mathcal{R}_\nu(g_\nu^*) = \mathbb{E}_{p_\nu(X_M)}[(g(X_M) - g_\nu^*(X_M))^2], \quad (14)$$

where $g_\nu^*(x_M) = \mathbb{E}_{p_\nu}[T | X_M = x_M]$. Applying equation 14 with $\nu = \text{t}$ and $g = \widehat{g}$ yields

$$\mathcal{R}_t(\widehat{g}) - \mathcal{R}_t(g_\text{t}^*) = \mathbb{E}_{p_\text{t}(X_M)}[(\widehat{g}(X_M) - g_\text{t}^*(X_M))^2].$$

Now write $g_t^* = g_s^* + \Delta$, so that pointwise in x_M ,

$$\hat{g} - g_t^* = (\hat{g} - g_s^*) - \Delta.$$

Expanding the square gives

$$(\hat{g} - g_t^*)^2 = (\hat{g} - g_s^*)^2 - 2(\hat{g} - g_s^*)\Delta + \Delta^2,$$

hence

$$(\hat{g} - g_t^*)^2 - (\hat{g} - g_s^*)^2 = -2(\hat{g} - g_s^*)\Delta + \Delta^2.$$

Taking absolute values and applying $|ab| \leq |a||b|$ yields the pointwise bound

$$|(\hat{g} - g_t^*)^2 - (\hat{g} - g_s^*)^2| \leq 2|\hat{g} - g_s^*||\Delta| + \Delta^2.$$

Finally, taking expectation under the target marginal $p_t(X_M)$ gives

$$\left| \mathbb{E}_{p_t(X_M)}[(\hat{g} - g_t^*)^2] - \mathbb{E}_{p_t(X_M)}[(\hat{g} - g_s^*)^2] \right| \leq 2 \mathbb{E}_{p_t}[|\hat{g}(X_M) - g_s^*(X_M)| |\Delta(X_M)|] + \mathbb{E}_{p_t}[\Delta(X_M)^2].$$

Substituting $\mathbb{E}_{p_t}[(\hat{g} - g_t^*)^2] = \mathcal{R}_t(\hat{g}) - \mathcal{R}_t(g_t^*)$ from equation 14 proves the claimed inequality.

If shifts occur only outside M , then $p_s(T | X_M) = p_t(T | X_M)$ and thus $\Delta \equiv 0$, which yields the stated exact identity. \square